ATTACHMENT II

FEASIBILITY STUDY OF INVENTORY TRENDING

METHODS WITH RC PUMPS OPERATING

OCTOBER 1982

Prepared by the
Babcock & Wilcox Company

for

Duke Power Company
Florida Power Corporation
Toledo Edison Company
Consumers Power Company
Sacramento Municipal Utilities Division

B&W Document ID. 77-1137950-00

TABLE OF CONTENTS

LIST OF SYMBOLS

SYMBOL	DEFINITION
A	Area
g_c	gravitation constant
H	pump head
I	current
K	flow coefficient
ΔP	pressure differential
PF	power factor
P_m	motor power
P_p	pump power
Q	volumetric capacity
T	pump torque
$\bar{V}$	velocity
V	voltage
v	specific volume
W	mass flow rate
x	quality
Y	net expansion factor
α	void coefficient
α_η	normalized pump speed
β	normalized pump torque
η_I	pump impeller efficiency
η_m	motor efficiency
η_p	overall pump efficiency
Ω	pump speed
ρ	density
ν_η	normalized pump flow
Subscripts or Superscripts	
G	gas phase
L	liquid phase
TP	two-phase
f	saturated liquid
g	saturated gas
r,o	reference or calibrated state

1.0 INTRODUCTION

1.1 Summary

Subsequent to the accident at TMI-2, the NRC required a review of instrumentation to indicate the approach to and onset of inadequate core cooling. As a result, the owners of B&W nuclear power plants reviewed level measurement systems which would operate when the reactor coolant pumps were off. During industry meetings with the NRC staff in early 1982, the staff indicated that an indication of system inventory with reactor coolant pumps on was desired. This report provides the results of an investigation which demonstrate that either of two methods, a Gentile flow tube ΔP system or an RC pump current system using presently installed equipment as a base can provide satisfactory inventory trending information with the reactor coolant pumps operating.

1.2 Background

Following the TMI-2 accident, the capability to monitor the primary system water inventory was identified as a potentially useful accident management tool. Review of TMI-2 data and subsequent small break loss of coolant accident (SB LOCA) analyses[1,2] has revealed that continuous operation of the RC pumps during the transient resulted in a highly voided primary system. When the RC pumps were tripped in this condition, the liquid that was previously dispersed throughout the system via pumping action, collapsed to the low points of the primary system, such as the bottom of the reactor vessel and steam generators. Consequently, the low water inventory at the time of the pump trip could result in an insufficient level for adequate core cooling.

In the fall of 1979, the NRC made a generic assessment of delayed RC pump trips during a SB LOCA.[3] They concluded that due to the uncertainties involved in SB LOCA analysis the prudent course of action would be to trip the RC pumps immediately following an indication that a LOCA had occurred (RC pressure dropping below the HPI setpoint). It was also recognized that the immediate pump trip approach was less than optimum.

For example, in overcooling events (i.e., steam line break) which cause shrinkage of the primary system and loss of RC pressure, early RC pump trip (and subsequent loss of pressurizer spray) can aggravate these transients and extend the time required to bring the plant into a controlled shutdown conditon. However, since these transients did not lead to unacceptable consequences, early pump trip was adopted as a course of action.

Current procedures in existence on operating plants therefore call for manual trip of reactor coolant pumps when the HPI setpoint is reached. Even though the operators are now trained to trip the pumps, the NRC has requested the additional capability to trend inventory with the pumps operating. This report evaluates potential systems which could provide the trending information required.

1.3 Report Organization

In the next section, two methods for measuring primary system inventory which relate measurable physical quantities to RC voiding are presented. Since both methods rely on various assumptions concerning the performance of the RC system, Section 3 of this report is presented to substantiate these assumptions. This supporting data was obtained from the TMI-2 accident and various experiments conducted in the last ten years. After review of the supporting data, one preferred model is identified for each of the measurement methods. In Section 4, these models are compared such that the advantages and limitations of each measurement can be assessed. The potential use of these methods in the pump trip circuitry is discussed in Section 5 and the conclusions and recommendations are presented in Section 6.

2.0 PROPOSED METHODS FOR MEASURING INVENTORY

The mathematical representations of the relationship between RC voiding to Gentile ΔP and pump current are presented in this section of the report. Justification for the assumptions used to derive these models will be addressed in the next section, when the supporting data is reviewed. For each method, two mathematical models are developed to allow for a comparative description of the phenomena.

2.1 Gentile ΔP

A relationship has been shown between RC flow as measured by the Gentile flow tubes and system voiding for the TMI-2 accident. The data is presented in Figure 1. Visual inspection suggests that a linear relationship between system voiding and mass flow rate may exist. Upon further examination it was noted that the relationship between flow and density can be represented by:

$$W = \rho \bar{V} A = \rho Q$$

where

W = measured mass flow rate (lb/sec)

ρ = density (lb/ft^3)

$\bar{V}$ = fluid velocity (ft/sec)

A = cross section area (ft^2)

Q = volumetric flow rate (ft^3/sec)

If one assumes that the volumetric capacity of the RC pumps is not degraded in any way (i.e., Q is constant), a simple one-to-one relationship then exists between flow and density. Specifically, when comparing to a reference (subscript r) or calibrated condition:

$$\frac{W}{W_r} = \frac{\rho}{\rho_r} \qquad (1)$$

Equation 1 indicates that mass flow rate varies linearly with respect to density. Further, note that the thermodynamic representation for void can be expressed in terms of density as:

$$\alpha = \frac{\rho - \rho_f}{\rho_g - \rho_f} \qquad (2)$$

where ρ = two-phase density (lb/ft^3)

ρ_f = density of the saturated liquid (lb/ft^3)

ρ_g = density of the saturated gas (lb/ft^3)

α = void coefficient

Then, combining equation 1 and 2 will yield a final relationship between the measured flow rate as specified by the Gentile and the primary system voiding (α).

$$\alpha = \frac{(\frac{W}{W_r})\rho_r - \rho_f}{\rho_g - \rho_f} \qquad (3)$$

At a given saturation pressure, a linear relationship does exist between measured mass flow rate and system voiding.

Equation 3 represents one mathematical model for the phenomena seen in Figure 1, RC measured flow versus RC system voiding. However, this simplistic model fails to account for any variation in Gentile performance when two-phase conditions exist. In particular, will the Gentile function in the same manner in both single phase and two-phase flow conditions (i.e., will flow rate be proportional to the square root of the generated ΔP across the Gentile). Review of numerous papers concerning the measurement of various two-phase fluids

in venturis and orifices have revealed that this is not the case, i.e., ΔP metering devices have distinct two-phase characteristics which differ from those found during single phase operation.

The theory of two-phase flow characteristics through orifices, as developed by J. W. Murdock,[4] will provide the second model upon which the flow-density correlation can be explored. This theory was chosen because 1) its development is based on thermodynamic and hydrodynamic first principles, and 2) Murdock's work is referenced extensively in two-phase literature and thus forms somewhat of a standard. For the sake of completeness, an outline of his model will be repeated here.

The flow rate through a ΔP metering device can be expressed by:

$$W = AKY\sqrt{2g_c \Delta P \rho} \qquad (4)$$

where
- W = mass flow rate (lb/sec)
- A = cross section area (ft^2)
- K = flow coefficient which includes the velocity of approach factor
- Y = net expansion factor
- g_c = gravitational constant (32.174 lb-ft/lb_f-sec^2)
- ΔP = pressure differential across device (lb_f/ft^2)
- ρ = fluid density (lb/ft^3)

Noting that $Y = 1.0$ for the incompressible liquid phase, a set of equations representing all phase conditions can be written.

Single Phase

$$W_L = AK_L \sqrt{2g_c \Delta P_L \rho_L} \quad (5)$$

$$W_G = AK_G Y_G \sqrt{2g_c \Delta P_G \rho_G} \quad (6)$$

Two-Phase

$$W_L = A_L (K_L)_{TP} \sqrt{2g_c \Delta P_{TP} \rho_L} \quad (7)$$

$$W_G = A_G (K_G Y_G)_{TP} \sqrt{2g_c \Delta P_{TP} \rho_G} \quad (8)$$

Equation 5 and 6 are representative forms of equation 4 for the single phase flow of liquid and steam, respectively. Equations 7 and 8 govern during two-phase flow conditions when both components are present in the mixture. The new variables are defined as follows:

W_L = liquid phase flow rate (lb/sec)

W_G = gas phase flow rate (lb/sec)

A_L = area which the liquid phase occupies (ft^2)

A_G = area which the gas phase occupies (ft^2)

K_L, K_G, $(K_L)_{TP}$, $(K_G)_{TP}$ = flow coefficient for liquid, gas, liquid in two-phase, and gas in two-phase conditions, respectively.

Y_G, $(Y_G)_{TP}$ = net expansion coefficient for the gas in single and two-phase conditions, respectively.

ΔP_L, ΔP_G, ΔP_{TP} = pressure differential for liquid, gas, and two-phase conditions, respectively. (lb_f/ft^2)

ρ_L, ρ_G = density of liquid and gas phases, respectively (lb/ft^3)

By combining equations 5-8 and representing the ratio of component flows by quality (x), Murdock derived a single expression for flow as a function of the two-phase ΔP measurement.

$$W = \frac{(K_G Y_G)_{TP} \, A \sqrt{2 g_c \, \Delta P_{TP} \, \rho_G}}{x + \frac{(1-x)\,(K_G Y_G)_{TP}}{(K_L)_{TP}} \sqrt{\frac{\rho_G}{\rho_L}}} \qquad (9)$$

Murdock conducted many experiments with various orifices and fluids and concluded that $K_L/(K_L)_{TP} = 1.26$ and $K_G Y_G/(K_G Y_G)_{TP} = 1.0$. The physical significance of these coefficients is important. Since the gas flow coefficient ratio is unity, the presence of the liquid phase has no effect on the ability of the orifice to pass the gas phase through the available area, A_G. However, the liquid flow coefficient ratio is 1.26, signifying that the presence of the gas phase will effectively reduce the liquid flow by $\sim$ 20% of the value expected (provided ΔP_{TP} and ρ_L remain fixed).

To apply the theory presented above to the problem of correlating RCS flow to voiding, the following assumptions were made:

1. The theory is applicable to any ΔP flow meter.

   The literature revealed that this theory can be applied to orifices or venturis. Gentile flow tubes, orifices, and venturis are all ΔP metering devices and, therefore, the generic theory presented by Murdock should apply equally for all of these devices.

2. The gas and liquid flow coefficient ratios are both unity.

   The coefficients found by Murdock where unity and 1.26 for the gas and liquid phase, respectively; however, the water - steam data covered the range of $80\% < x < 100\%$. The range of interest when measuring RCS voiding to determine pump trip

is 0%<x<5% (0% <α< 70%). Therefore, a literature search was conducted to find realistic flow coefficient ratios in the low quality regime. An extensive study conducted by the Atomic Energy of Canade Limited (AECL)[5] was found to provide such data. Tnis data was obtained for the low quality regime (5%< x <50%) at pressures of interest (1200 psig). The results are as follows:

Device	Diameter Ratio(β)	$\frac{K_G Y_G}{(K_G Y_G)_{TP}}$	$\frac{K_L}{(K_L)_{TP}}$
Orifice	0.45	1.0372	1.0789
Orifice	0.70	1.0818	0.9999
Venturi	0.58	1.0427	1.0779

Review of equation 9 reveals that $(K_L)_{TP}$ must approach K_L as quality tends to zero. Considering this boundary condition and the AECL data presented above, a valid estimate for the gas and liquid flow coefficient ratios is unity. This approach will avoid the discontinuity at the saturation line.

3. The flow coefficient of the Gentile will be the same for both phases.

The flow coefficients of the gas and liquid phase should be approximately equal for the Gentile since impulse nozzles are used to measure the resulting ΔP. These nozzles measure fluid kinetic energy and are not sensitive to the phase of fluid being measured.

At sufficiently high Reynolds numbers, tests[6] have shown that the Gentile displays a constant flow coefficient for liquid flow. However, this value diminishes slightly at low Reynolds numbers. Consequently, one would expect that the gas flow coefficient will degrade somewhat in the low quality regime at corresponding low Reynolds numbers. Murdocks data reveals that this effect is not large and, therefore, it will be assumed that equal flow coefficients exist.

4. The net expansion factor is unity.

The range of steam velocities expected are completely subsonic and hence, no compressibility effects must be included. Consequently, the next expansion factor can be set to unity.

If the four assumptions listed above are combined with the assumption of constant flow capacity, (as used in the development of the first model), the development of a second correlation is as follows:

$$\frac{W}{W_r} = \frac{\rho_{TP}}{\rho_r} \quad \text{(as presented earlier in equation 1)}$$

Since equation 9 provides an expression for the two-phase flow (W), it can be inserted into the relation above yielding.

$$\frac{(K_G Y_G)_{TP} \quad A\sqrt{2g_c \Delta P_{TP} \rho_G}}{x + \frac{(1-x)(K_G Y_G)_{TP}}{(K_L)_{TP}} \sqrt{\frac{\rho_G}{\rho_L}}} = W_r \, (\rho_{TP}/\rho_r) \qquad (10)$$

Applying the simplifying assumptions concerning the flow coefficients and the net expansion factor will permit reduction of the left-hand side of equation 10. At this time, it should be emphasized that the liquid and gas components are actually saturated water existing in two distinct phases. Therefore, the standard subscripts f and g for the liquid and vapor phase properties can be used to replace the L and G subscripts used previously.

Equation 10 can now be rewritten:

$$\frac{KA\sqrt{2g_c\Delta P_{TP}\rho_g}}{x + (1-x)\sqrt{\rho_g/\rho_f}} = W_r\,(\rho_{TP}/\rho_r) \qquad (11)$$

In the above equation, a single flow coefficient, K, is used since it was assumed that all flow coefficients are identical. The two-phase density on the right-hand side of equation 11 can be expressed as:

$$\rho_{TP} = 1/v_{TP} = (v_f\,(1-x) + v_g x)^{-1} \qquad (12)$$

also, at the time of Gentile calibration:

$$W_r = KA\sqrt{2g_c\Delta P_r/v_r} \qquad (13)$$

Substitution of equation 12 and 13 into equation 11 yields an expression for quality as a function of two-phase Gentile ΔP.

$$\frac{\sqrt{\frac{\Delta P_{TP}}{v_g}}}{x + (1-x)\sqrt{\frac{v_f}{v_g}}} = \frac{v_r\sqrt{\frac{\Delta P_r}{v_r}}}{v_f(1-x) + v_g x} \qquad (14)$$

Or after expanding and collecting terms:

$$X = \frac{\sqrt{\frac{v_r}{v_g}}\sqrt{\frac{\Delta P_{TP}}{\Delta Pr}}\left(\frac{v_f}{v_r}\right) - \sqrt{\frac{v_f}{v_g}}}{\left[1 - \sqrt{\frac{v_f}{v_g}} + \sqrt{\frac{v_r}{v_g}}\sqrt{\frac{\Delta P_{TP}}{\Delta Pr}}\ \frac{(v_f - v_g)}{v_r}\right]} \qquad (15)$$

Assuming no interfacial slip:

$$\alpha = \frac{1}{1 + \frac{v_f}{v_g}\ \left(\frac{1-x}{x}\right)} \qquad (16)$$

Equations 15 and 16 form the relationship governing the measured ΔP of the Gentile and RCS voiding. The required inputs are:

1. RCS pressure to determine v_f and v_g.
2. Gentile ΔP signal which is used as the ΔP_{TP} input.
3. The ΔP measurement from the Gentile when it is calibrated using the secondary side heat balance (ΔP_r input).
4. The specific volume determined at the time of Gentile calibration (v_r).

2.2 PUMP CURRENT

Two mathematical models can be developed which relate pump current to RCS voiding. Each model is formed using an expression for the energy transference from the pump to the coolant.

The input three-phase power, P_m, required to drive a constant speed (constant frequency) squirrel cage induction motor can be expressed as follows:

$$P_m = \sqrt{3}\, IV\,(PF) \tag{17}$$

where $\sqrt{3}$ = accounts for the 3-phase input of power

I = line current (RMS Amps)

V = line voltage (RMS volts)

PF = power factor (accounts for energy lost in setting up the magnetic field)

Similarly, the power, P_p, required to drive a pump can be expressed by considering the development of head:

$$P_p = \frac{\rho Q H}{\eta_p} \tag{18}$$

where ρ = fluid density (lb/ft^3)

Q = volumetric flow (ft^3/sec)

H = head generated by the pump (ft)

η_p = overall pump efficiency (accounts for the mechanical friction at the seals and bearings, hydraulic friction at the impeller vanes and the diffuser vanes, and various other hydraulic losses due to eddy formation.

If one accounts for the windage and mechanical friction losses of the motor by considering the motor efficiency, η_m, the transfer of power to the pump can be stated.

$$\eta_m P_m = P_p$$

or, inserting the previous definitions,

$$\eta_m \sqrt{3}\ IV\ (PF) = \frac{\rho QH}{\eta_p} \tag{19}$$

The change in current relative to varing fluid density can be addressed by denoting a reference point (^{o} superscript) condition.

$$\frac{\rho}{\rho^o} = \frac{\eta_p\ \eta_m\ IV\ (PF)\ Q^oH^o}{\eta_p{}^o\ \eta_m{}^o\ I^oV^o\ (PF)^o\ QH} \tag{20}$$

Assuming that the motor efficiency, voltage, power factor, capacity, and head remain constant, a simple relationship results.

$$\frac{\rho}{\rho^o} = \left(\frac{I}{I^o}\right)\left(\frac{\eta_p}{\eta_p{}^o}\right) \tag{21}$$

Inserting an expression relating void to density,

$$\rho = \rho_f - \alpha\ (\rho_f - \rho_g)$$

will yield the desired relationship between voiding and current.

$$\alpha = \frac{\rho_f - \rho^o \left(\frac{I}{I^o}\right)\left(\frac{\eta_p}{\eta_{p^o}}\right)}{\rho_f - \rho_g} \qquad (22)$$

A second model can be developed by considering the transference of torque within the pump. In this situation,

$$P_p = \frac{T\Omega}{\eta_I} \qquad (23)$$

where T = hydraulic torque transferred from the impeller to the fluid ($ft\text{-}lb_f$)

Ω = pump speed (rpm)

η_I = pump efficiency accounting for the mechanical friction at the seals and bearings, hydraulic friction and eddy losses within the impeller. Hydraulic friction and eddy losses within the diffuser vanes are not included since only power transfer at the impeller is being considered.

Coupling equation 23 with the homologous or normalized relation for torque,

$$\frac{T}{T_R} = \beta \left(\rho/\rho_R\right)$$

yields,

$$P_p = \beta T_R \rho \Omega / \eta_I \rho_R$$

Where β = normalized torque

T_R = rated torque (ft-lb_f)

ρ_R = density corresponding to T_R (lb/ft^3)

Assuming that the motor efficiency, voltage, power factor, and operating point of the pump (β,Ω) remain constant, a normalized relationship results.

$$\frac{\rho}{\rho^o} = \left(\frac{I}{I^o}\right) \left(\frac{\eta_I}{\eta_I{}^o}\right) \tag{24}$$

As before,

$$\alpha = \frac{\rho_f - \rho^o \left(\frac{I}{I^o}\right) \left(\frac{\eta_I}{\eta_I{}^o}\right)}{\rho_f - \rho_g} \tag{25}$$

This completes the development of the mathematical models. The four relationships involving gentille ΔP and void fraction, and pump current and void fraction are shown in Table 1.

TABLE 1: VOIDING MODELS

Gentile ΔP

Model 1:

$$\alpha = \frac{\sqrt{\frac{\Delta P_{TP}}{\Delta P_r}}\ \rho_r - \rho_f}{\rho_g - \rho_f} \tag{26}$$

Model 2:

$$x = \frac{\sqrt{\frac{v_r}{v_g}}\ \sqrt{\frac{\Delta P_{TP}}{\Delta P_r}}\ \left(\frac{v_f}{v_r}\right) - \sqrt{v_f / v_g}}{\left[1 - \sqrt{v_f / v_g} + \sqrt{\frac{v_r}{v_g}}\ \sqrt{\frac{\Delta P_{TP}}{\Delta P_r}}\ \frac{(v_f - v_g)}{v_r}\right]} \tag{27}$$

$$\alpha = \left[1 + \frac{v_f}{v_g}\ \left(\frac{1-x}{x}\right)\right]^{-1} \tag{28}$$

Pump Current

Model 1:

$$\alpha = \frac{\rho_f - \rho^o \ (I/I^o) \ (\eta_p/\eta_{p^o})}{\rho_f - \rho_g} \tag{29}$$

Model 2:

$$\alpha = \frac{\rho_f - \rho^o \ (I/I^o) \ (\frac{\eta_I}{\eta_{I^o}})}{\rho_f - \rho_g} \tag{30}$$

In summary, these models were based on the following assumptions:

Gentile ΔP, Model 1

1. The volumetric capacity of the pumps will not degrade.
2. The performance of the Gentile flow tube is the same in both single and two-phase flow.

Gentile ΔP, Model 2

1. The volumetric capacity of the pumps will not degrade.
2. The flow coefficient of the Gentile will be the same for both phases.

Pump Current, Model 1

1. The motor efficiency, voltage, and power factor remain constant.
2. The pump capacity and head do not degrade.

Pump Current, Model 2

1. The motor efficiency, voltage, and power factor remain constant.
2. Pump speed remains constant.
3. The hydraulic torque does not degrade.

The validity of these assumptions will be discussed further in Section 3.0 when the supporting data is presented.

FIGURE 1
% RC FLOW VS % VOIDS
DURING TMI-2 ACCIDENT

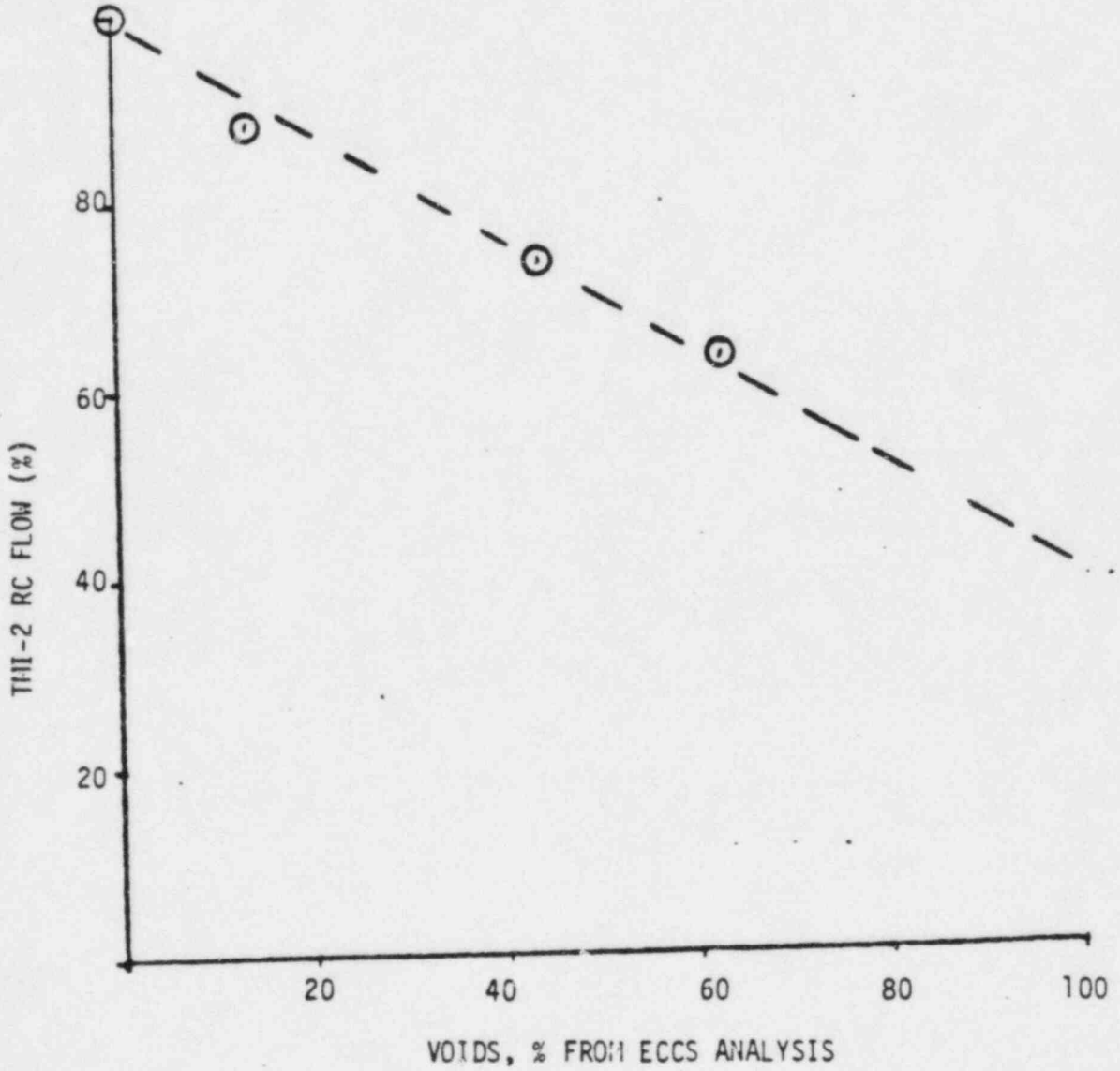

3.0 SUPPORTING DATA

To utilize the models developed in the last section, supporting data must be found to substantiate the assumptions used to develop the models. Consequently, a literature survey was conducted. This section of the report summarizes the findings of this study.

Review of the assumptions tabulated at the end of Section 2 reveals that supporting data is needed in three major areas. The first area concerns the questionable performance of the gentille under two-phase conditions. Specifically, does the theory presented by Murdock hold true or will a simpler approach suffice? If Murdock's theory does hold, will the flow coefficients of the liquid and gas phase be equal, or will slip between the phases produce erroneous results, etc.? Secondly, the characteristics of the pump drive motor must be examined. The variation in efficiency, voltage, speed, and power factor must be explored. In the last area, the performance of the pump under two phase conditions must be examined. This is a crucial topic since all of the models presented thus far rely on non-degraded pump performance (head, capacity, and torque).

In the review of Gentile literature, sparse information was found concerning single phase flow performance, and no information was found concerning two phase flow through Gentiles. In fact, the data obtained during the TMI-2 accident may represent the only two-phase performance information available for Gentiles. Therefore, the two models were applied directly to the TMI conditions and the results were compared with an estimate of system voiding made by ECCS analysis (Table 2 and Figure 2). In the ECCS computation, the CRAFT 2 computer

code was used with best-estimate inputs regarding makeup and letdown flows, leakage flows, and heat transmission throughout the RCS.

Each heading of Table 2 should be explained:

RCS Pressure - Value taken from ECCS analysis. (Since voiding is pressure dependent, the CRAFT 2 value must be used to maintain consistency.)

Measured flow rate - flow rate measured at TMI-2 via the Gentile

ΔP Gentile - calculated using typical conversion formula:

$$\text{LOOP flow (MPPH)} = 13.68 \sqrt{\Delta P \text{ (psid)}}$$

where MPPH = million pounds per hour

α_1 - voiding as estimated by Gentile - model 1

α_2 - voiding as estimated by Gentile - model 2

By examining Figure 2, the following can be concluded:

1. The fluctuating Gentile signal produces a false indication of voiding during the first 10 minutes of the transient. This is brought about by a combination of reasons:
   - i) accuracy of the Gentile
   - ii) speed cycling of the RC pumps due to asymmetric void formation within the loops
   - iii) abrupt addition of auxiliary feedwater at 8 minutes into the transient producing shrinkage of the primary system.
2. Model 1 for the Gentile produces diverging results when compared to the ECCS analysis.
3. Model 2 for the Gentile agrees favorably with the ECCS prediction when the transient settles out at 25-30 minutes.

This model predicts voiding to a lesser extent than the CRAFT 2 estimate, which may be the result of interfacial slip between the phases or a slightly degraded flow coefficient for the gas phase as explained earlier. In either case, the flow is over stated and hence the voiding estimate is low.

To summarize, the second Gentile model will relate Gentile ΔP to system voiding when the RCS is in a quiescent two-phase mode with pumps running. The first model does not account for any two-phase effects and, therefore, produces erroneous results. Consequently, this model will not be considered further in this study.

Figure 3 displays the operating characteristics of a typical pump drive motor. Considering the density variation associated with voiding to be on the order of 0 to 40%, the operating range of interest lies between 6000 and 10000 HP. In this range, when a constant voltage is supplied (6600 volts in this case), motor efficiency and power factor vary by less than ½%. As a result, current varies linearly with power in this range as shown in figure 3.

The variations in pump speed are small as load changes. Typically, the induction motor can generate 1000 HP for every rpm off synchronous. Therefore, the pump speed can be assumed to be essentially constant when compared to the 1200 rpm synchronous motor speed.

The assumptions of constant motor efficiency and power factor imply constant supply voltage. It is recognized that off normal voltages may occur due to bus transfers, pump starts or grid disturbances. These perturbations are expected to be of short duration and would

not have a significant impact on the use of pump current for inventory trending indication. Application of this measurement for alarm or pump trip circuits would require provisions for delaying the alarm or trip signal to avoid spurious actuations.

Operating characteristics of the pump drive motor in the range of interest can be summarized as follows:

1. The motor efficiency remains constant.
2. The power factor remains constant.
3. The pump speed remains constant.

Experimental data has been generated concerning the performance of the pumps under two-phase conditions. These experimental studies are summarized below.

Combustion Engineering, Inc./EPRI

In an effort to refine the analytical model of the reactor coolant pumps under hypothetical large break LOCA conditions, Combustion Engineering constructed a test system which utilized a 1/5 scale pump. Steady state tests were conducted near the operating point ($\nu_n/\alpha_n = 1.0$) and the results are presented in Figures 4 and 5. (Note ν_n is defined as the ratio of the actual flow rate to the rated flow rate and α_n is the ratio of the actual speed to rated speed.) For low void fraction (0-0.1), the pump head (Figure 4) remained at, or slightly above the water or non-degraded value. At 0.15 void, the head degrades almost linearly until the worst case (20% of the water value) is reached at .75 void.

Head then recovers as the single phase steam region is reached. A similar behavior is seen concerning torque, (see Figure 5), but the degradation is less severe. The degradation in head and torque at low pressures is even more pronounced due to the larger density differences between the steam and the liquid. Losses associated with these two-phase mechanisms are three times greater at 500 psia than at 1000 psia.

Babcock & Wilcox Company/EPRI

With the same program objectives, B&W constructed a test apparatus to analyze the performance of a 1/3 scale pump using air/water mixtures to simulate voiding. The results of these experiments are presented in Figures 6 and 7. Restricting our attention to the region around the operating point ($\nu_n/\alpha_n = 1.0$), the same degradation behavior is seen relative to the Combustion Engineering data. However, the degradation effects are exaggerated due to two-phase losses resulting from the large density difference between air and water.

CREARE Inc./EPRI

CREARE Inc. worked in parallel with the two studies mentioned above. In their test rig, a 1/20 scale pump was installed to address the effects of scaling. Figures 8 and 9 show the results of the tests conducted near the operating point for low pressure water/air mixtures. These results compare quite favorably with the B&W data presented earlier.

LOFT Research

As part of the Loss-of-Fluid Test (LOFT) Program, RC pump motor power and current measurements, and their utility as indicators of RCS

inventory is being explored. Current research shows a large head degradation at approximately 20% void (See Figure 10). This phenomena is consistent with the other data presented thus far for scaled pumps. It is interesting to note, that power and current measurements made during this transient (See Figures 11 and 12, respectively) do not exhibit the same discontinuity.

The following can be summarized concerning two-phase degradation of pumps:

1. In all cases, torque did not degrade as appreciably as developed head. This implies that larger losses occur in the diffuser section of the pump than in the impeller section. The LOFT data presented in Figures 10 through 12 shows that this is the case, with the impeller efficiently imparting hydraulic torque to a two-phase fluid at a homogeneous density, while the head abruptly degrades due to two-phase losses in the diffuser section.
2. All degradation effects are minimized at pressures above 1000 psia. This is important since the application of the void measurement will usually be made at elevated pressures (> 1000 psia).
3. Review of the RCS flow for the TMI-2 event reveals that little if any pump capacity degradation occurred. Therefore, it must be concluded that scaling effects have not been adequately addressed by the pump testing summarized in this study. The probable cause for this discrepancy deals with the inability of these tests to scale the bubbles such that the relationship between the size of the bubbles with respect to the vane spacing on the impeller and diffuser is preserved. For example, if ping-pong balls were

suspended in a fluid system, their presence would choke a small pump, whereas a large pump would pass the balls virtually undetected.

4. In developing the technical approach for the pump current measurement, model 2 (based on torque transfer) is a stronger approach since only impeller dynamics are involved. Model 1 (based on head and capacity) would involve resolving the energy losses in the pump casing, thus making this approach less desirable. Therefore, model 1 will not be considered further.

The review of the data presented in this section has resulted in the elimination of two of the models developed in Section 2.0. The remaining two models will be discussed further and compared in the fourth section of this report.

TABLE 2

ESTIMATES OF TMI-2 SYSTEM VOIDING

Time (min)	RCS Pressure (psia)	Measured W ($lb/hr \times 10^6$)	ΔP Gentile (psid)	α_1 (Void)	α_2 (Void)
0	2186.55	67.4	24.274	0.000	0.000
1	1731.93	66.2	23.418	0.000	0.001
2	1638.45	65.8	23.136	0.008	0.022
3	1566.36	65.8	23.136	0.022	0.030
4	1503.86	65.6	22.995	0.034	0.042
5	1455.83	65.6	22.995	0.043	0.047
6	1498.91	64.9	22.507	0.049	0.057
7	1560.04	64.0	21.887	0.051	0.075
8	1616.37	63.5	21.546	0.051	0.074
9	1587.78	65.4	22.855	0.024	0.036
10	1548.81	66.4	23.559	0.012	0.020
15	1374.95	66.4	23.559	0.043	0.034
20	1206.94	66.0	23.276	0.080	0.063
25	1105.19	60.3	19.430	0.176	0.179
30	1104.37	59.5	18.917	0.187	0.194
35	1103.30	58.0	17.976	0.209	0.222
40	1103.57	56.0	16.757	0.239	0.259
45	1104.22	54.0	15.582	0.268	0.297
50	1104.89	53.0	15.010	0.283	0.315
55	1104.46	50.0	13.359	0.326	0.371
60	1075.98	58.0	12.311	0.358	0.409
65	1074.44	46.0	11.307	0.387	0.446
70	1067.31	44.5	10.582	0.412	0.473

FIGURE 2:

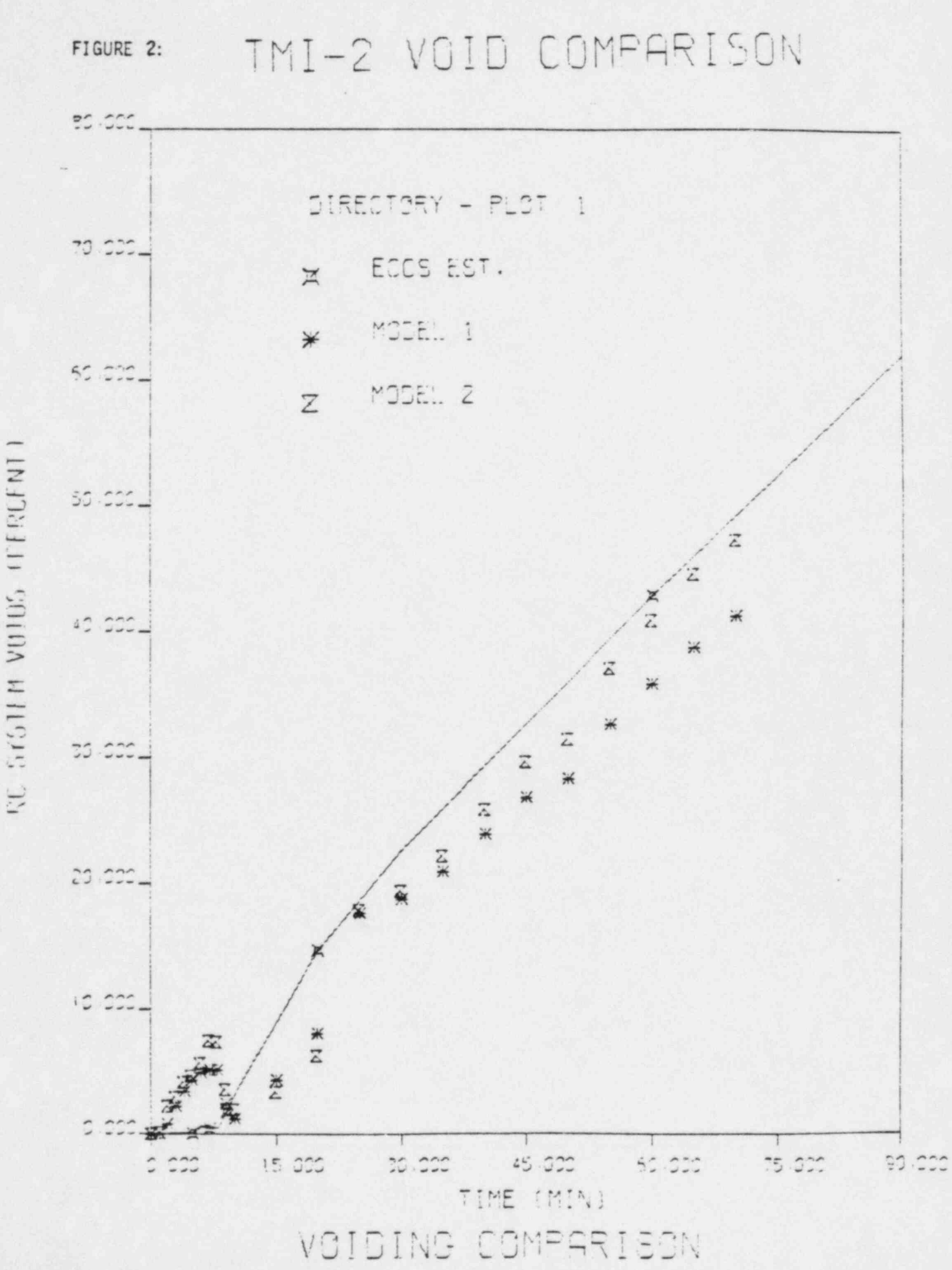
TMI-2 VOID COMPARISON
DIRECTORY - PLOT 1
ECCS EST.
MODEL 1
MODEL 2
TIME (MIN)
VOIDING COMPARISON

FIGURE 3: MOTOR CHARACTERISTICS

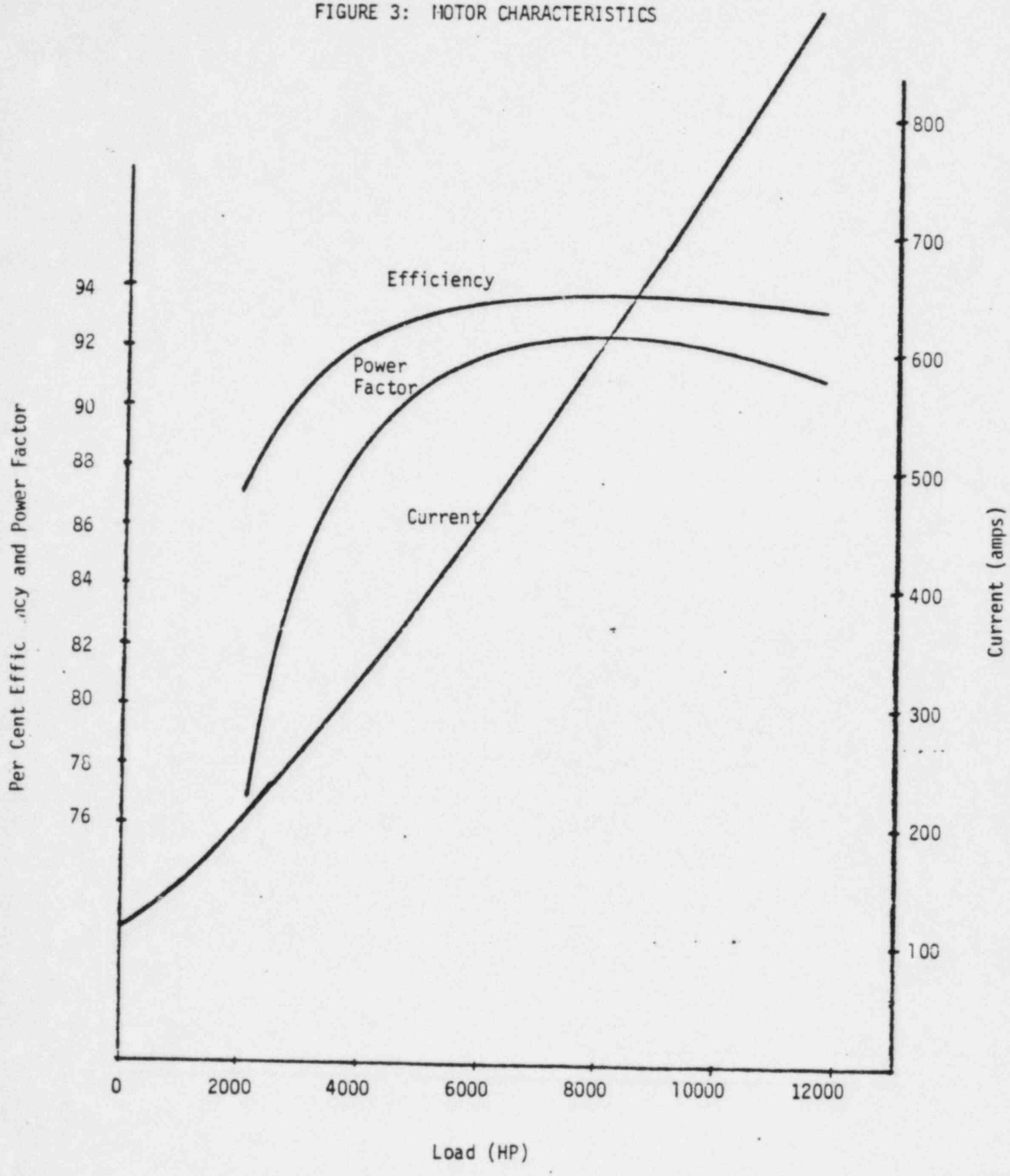

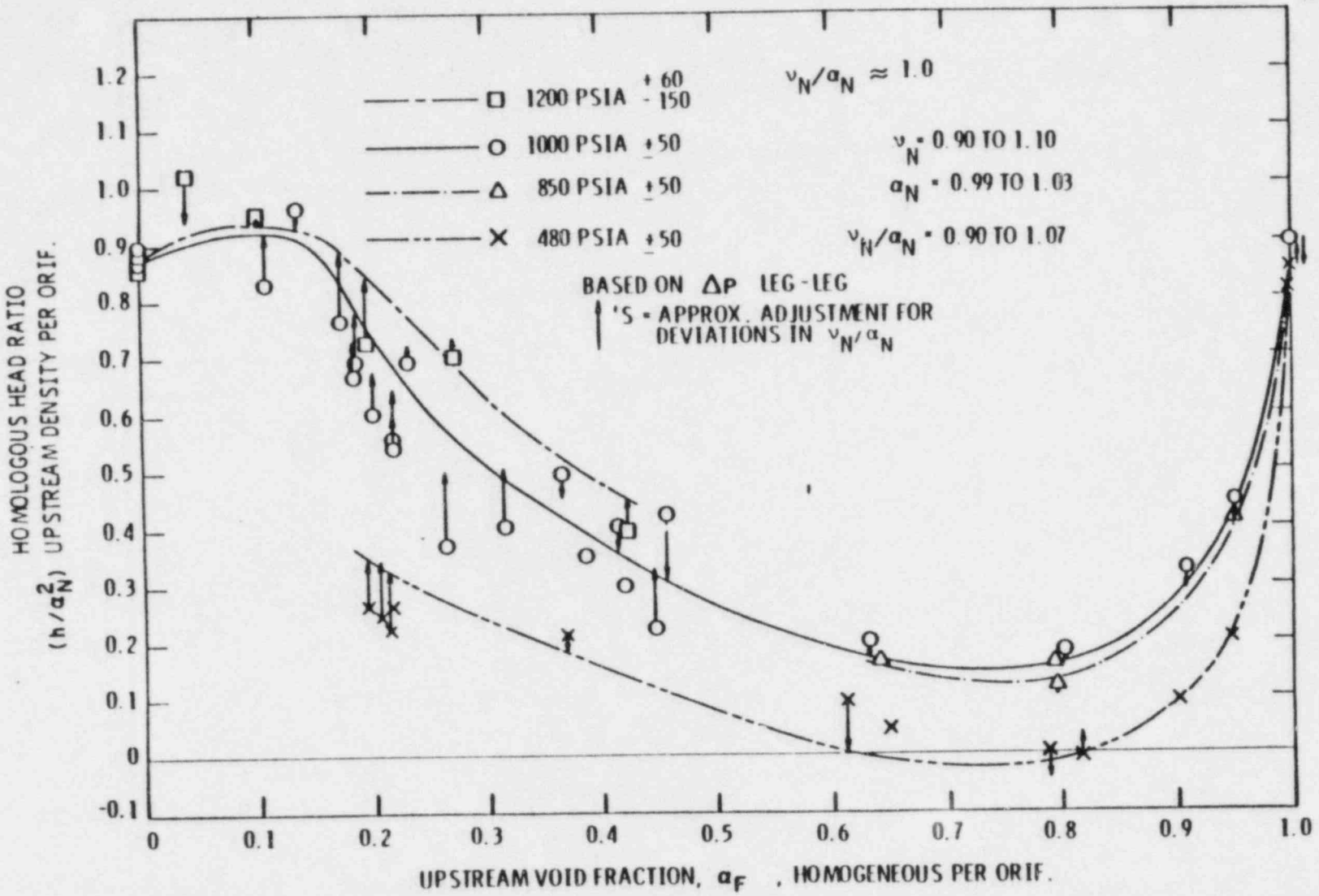

Figure 4: Effect of Void Fraction on Homologous Head Ratio Near Rated Flow and Speed

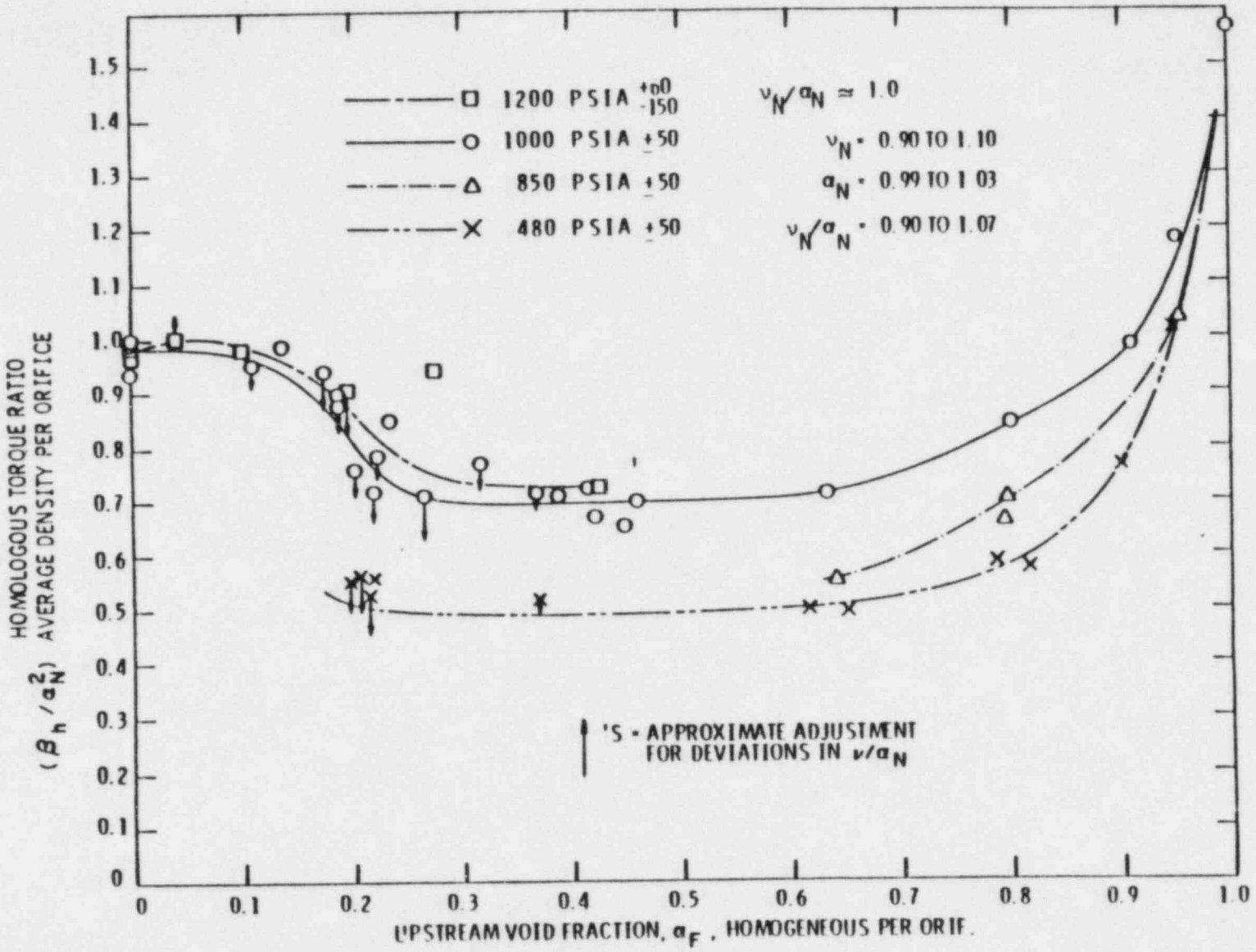

Figure 5: Effect of Void Fraction on Homologous Torque Ratio Near Rated Flow and Speed

FIGURE 6: Homologous Head at Various Pump Inlet Void Fractions for First-Quadrant Pump Operation

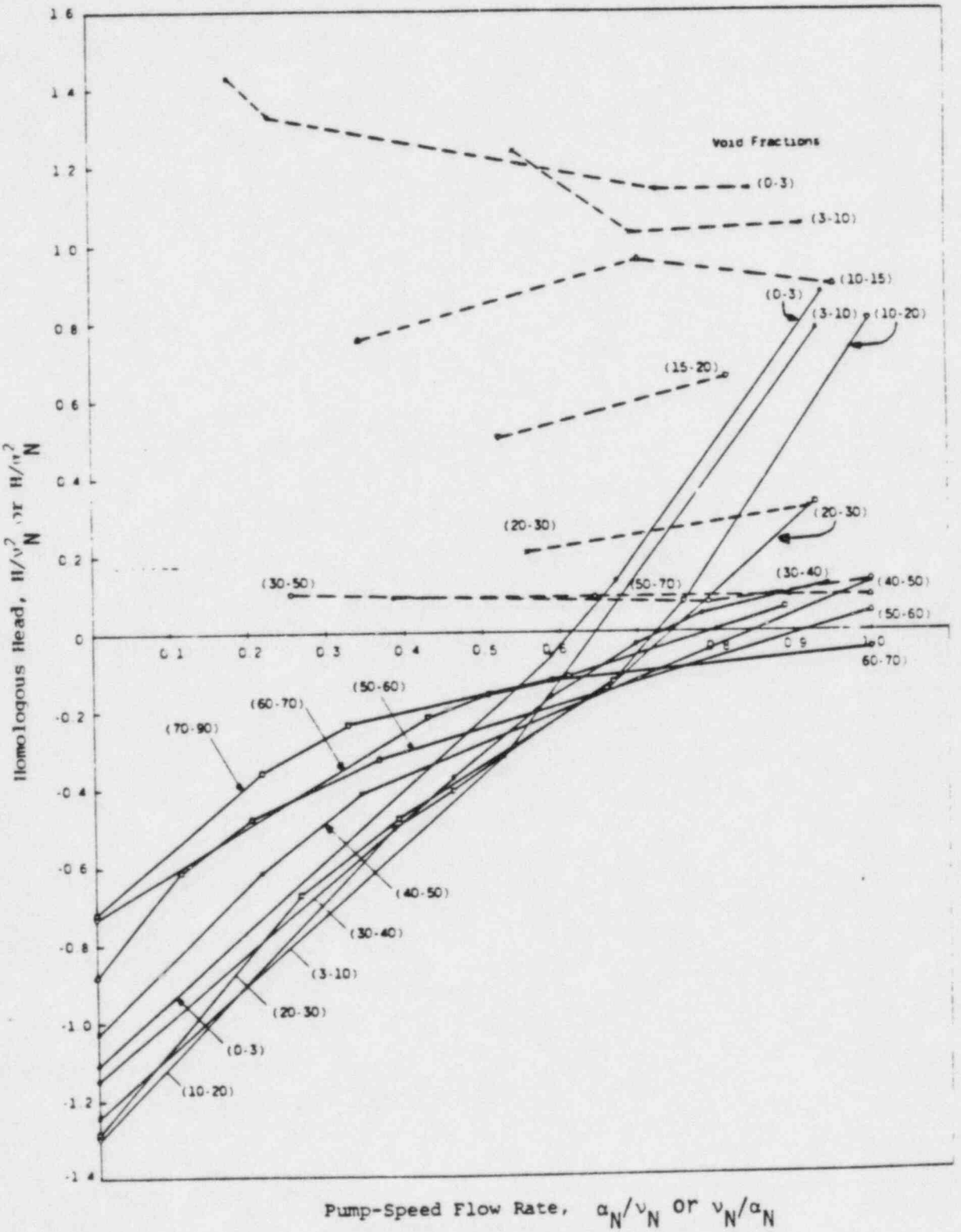

FIGURE 7: Homologous Torque at Various Pump Inlet Void Fractions for First-Quadrant Pump Operation

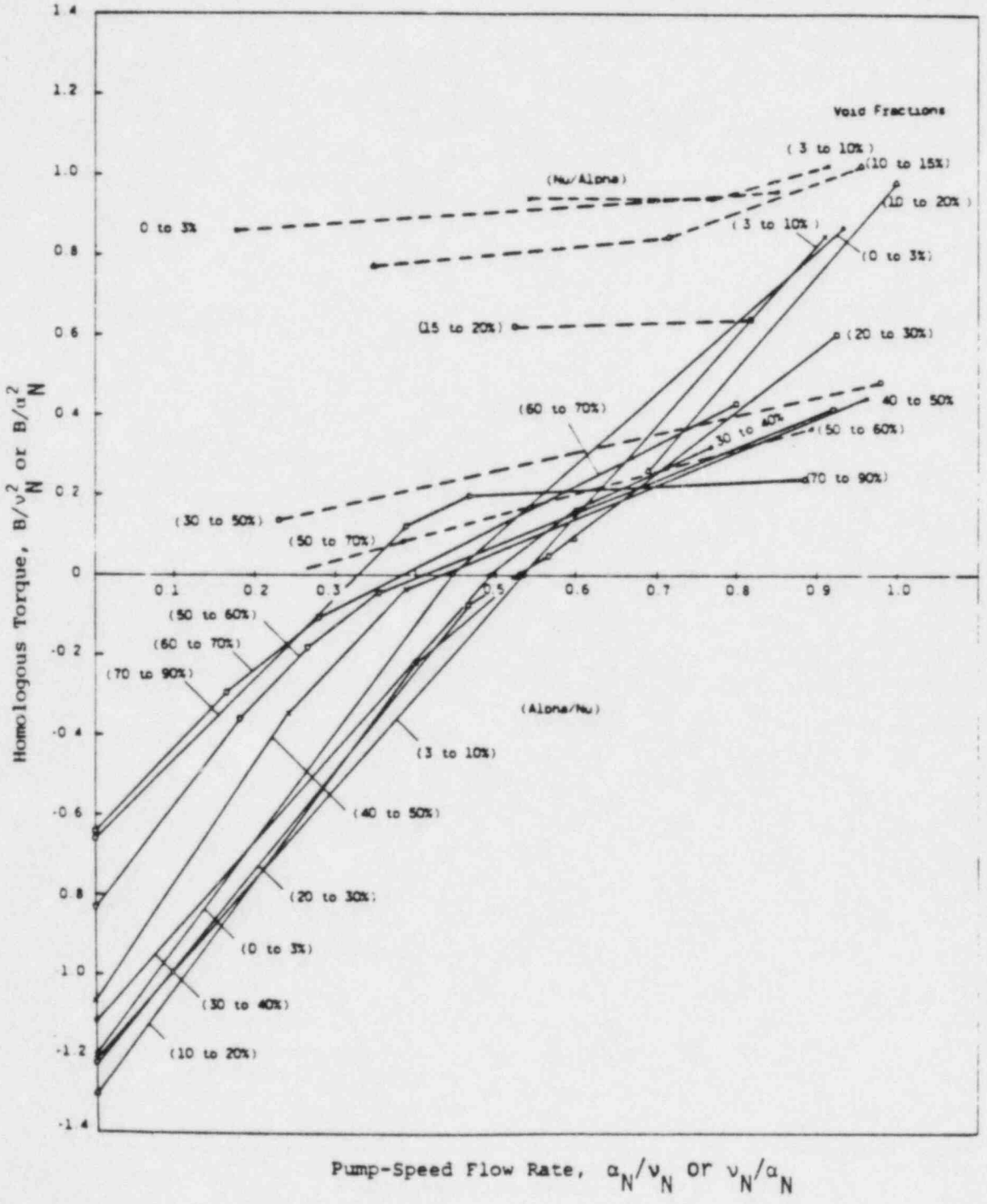

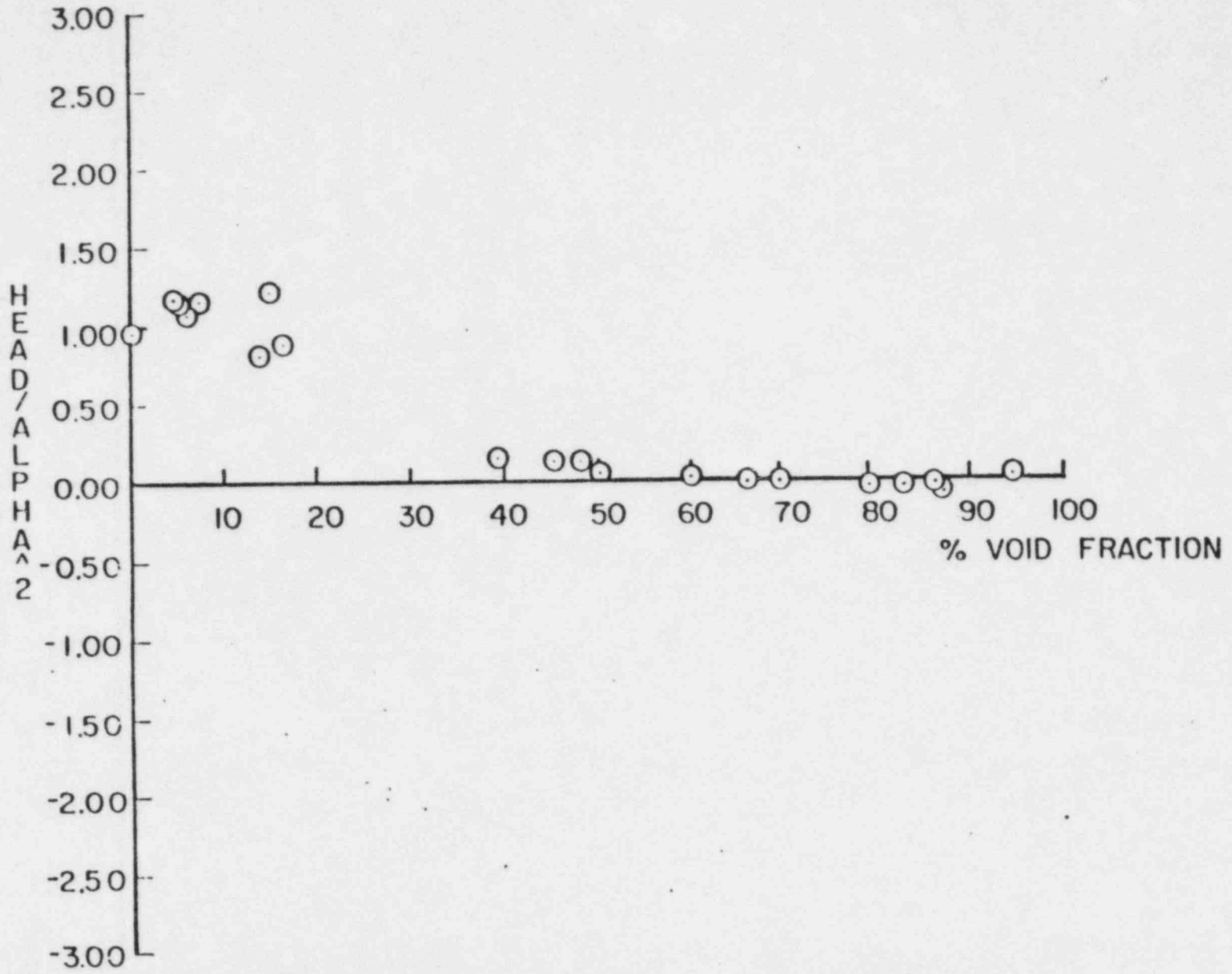

FIGURE 8: HEAD DEGRADATION VS. VOID FRACTION, FIRST QUADRANT, $\nu/\alpha_N = 0.9$

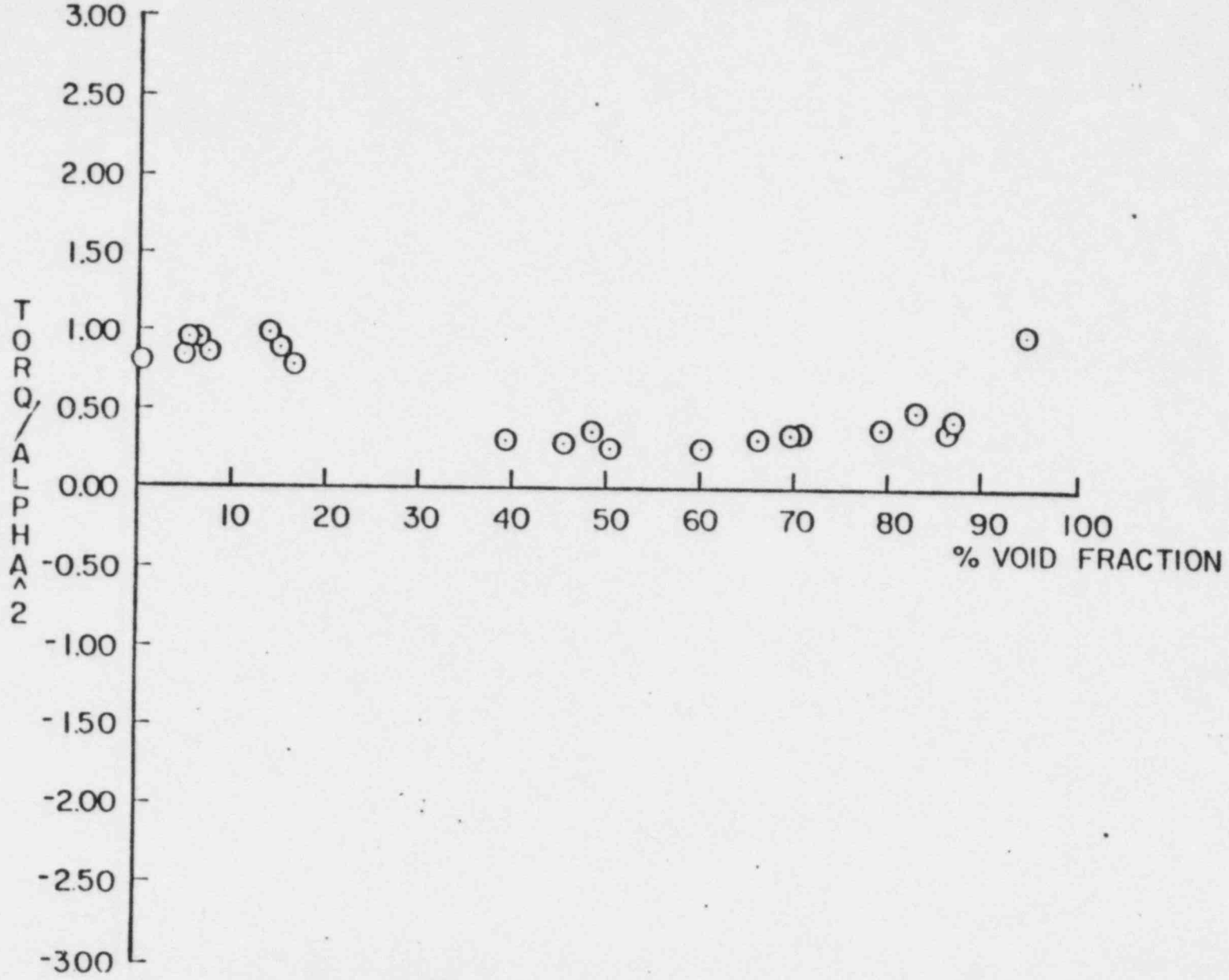

FIGURE 9: TORQUE DEGRADATION VS. VOID FRACTION, FIRST QUADRANT, $v/a_N = 0.9$

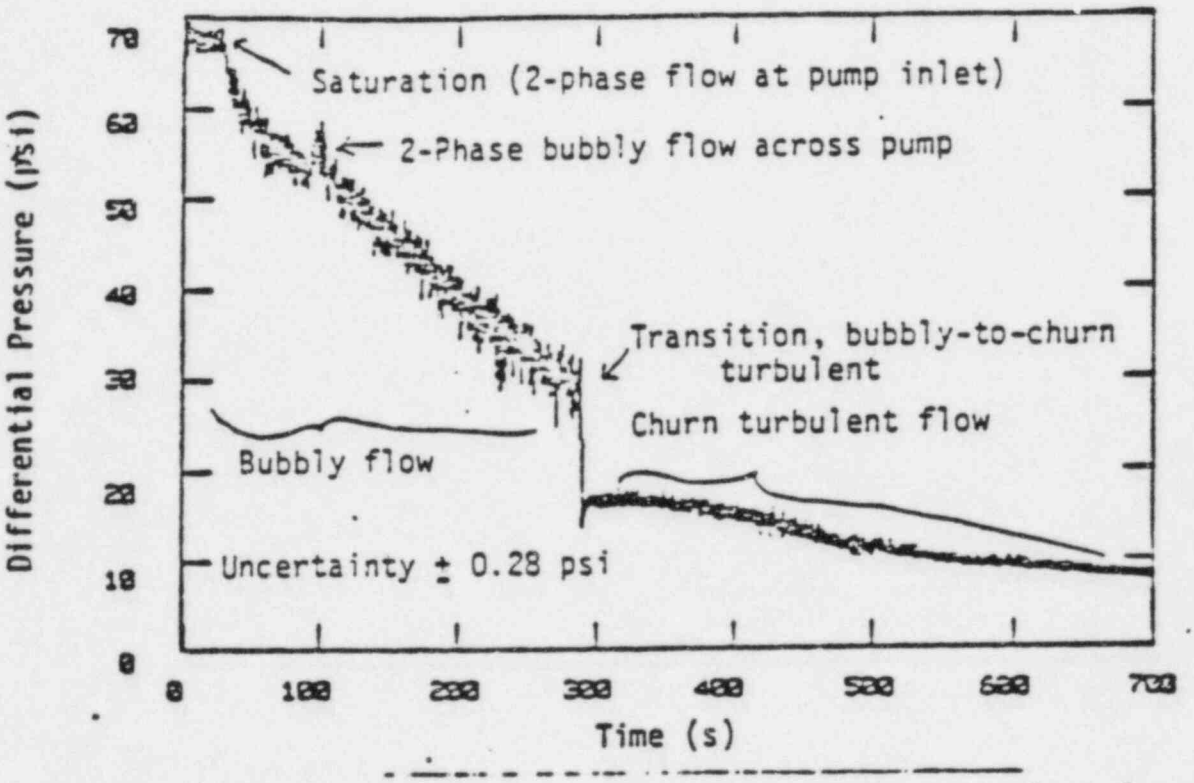

Figure 10: Differential Pressure Across Primary Coolant Pumps

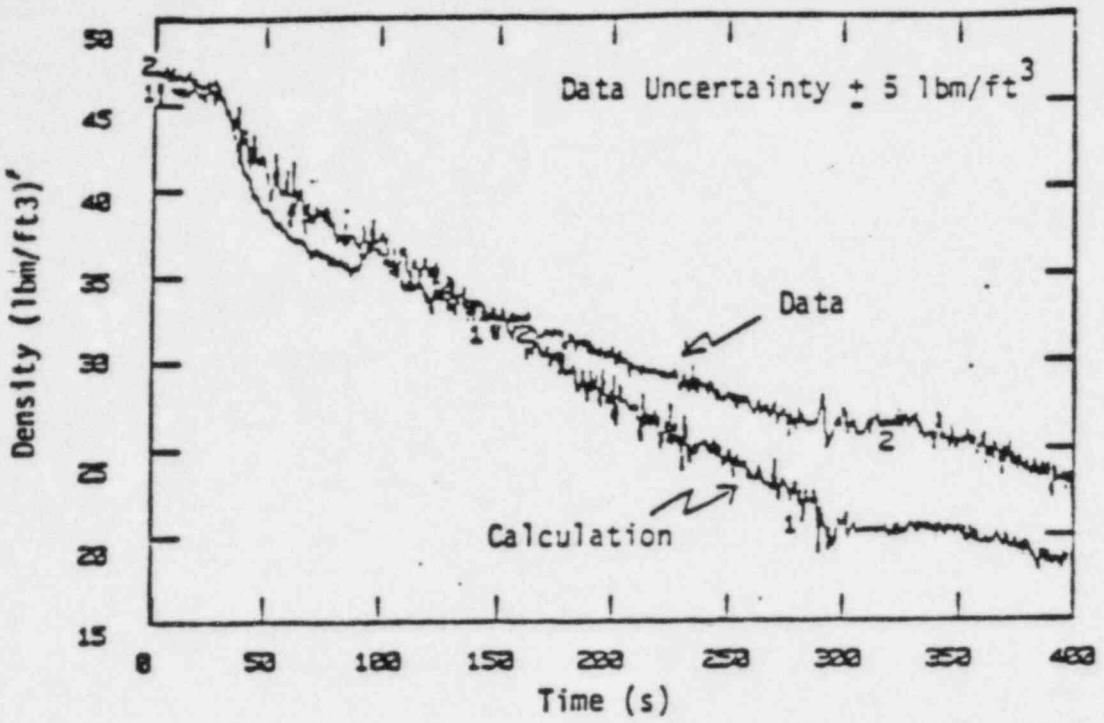

Figure 11. Measured Density Upstream of Pump Compared With Prediction Using Pump Motor Power Assuming Constant Volumetric Flow and Pump Head

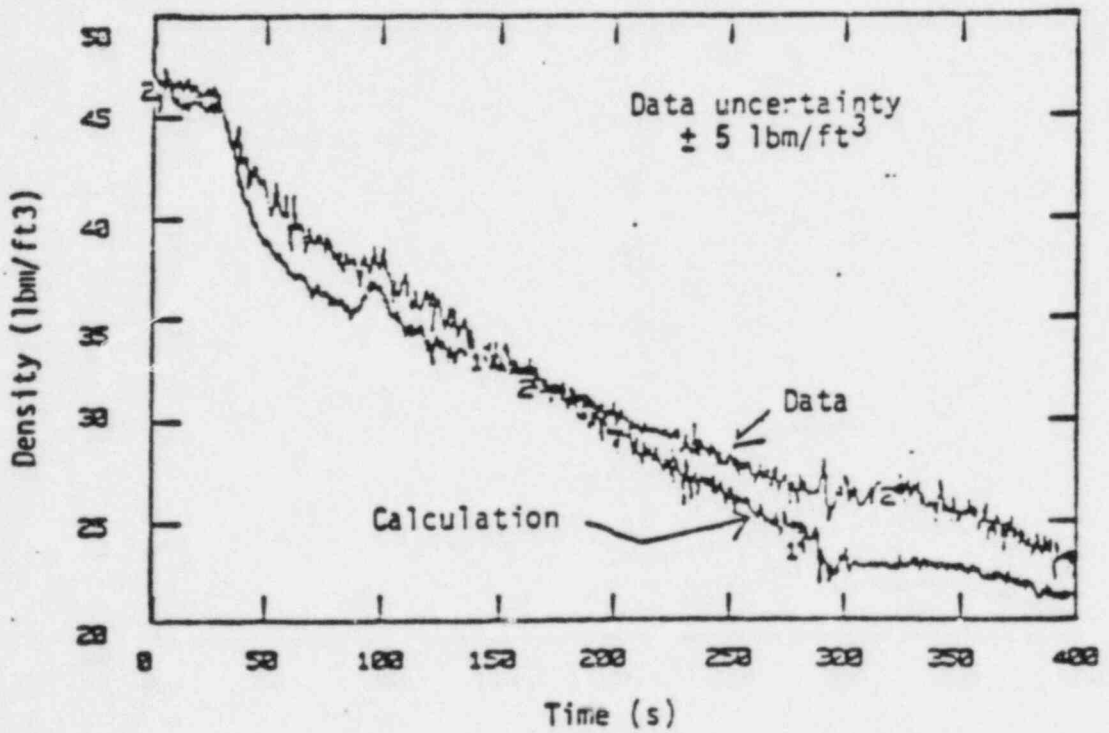

FIGURE 12. Measured Density Upstream of Pump Compared With Prediction Using Pump Motor Current Assuming Constant Volumetric Flow and Pump Head

4.0 Comparison of the Gentile ΔP and Pump Current Methods

After reviewing the data presented in the previous section, two inventory trending models remain as viable choices. The first model involves correlating the Gentile ΔP with the system voiding. Murdock's theory of two-phase flow through ΔP meters forms the basis of this approach. The second model uses a correlation between pump current and system voiding. The transfer of torque from the impeller to the fluid forms the basis of this model. The advantages and limitations of the models can be compared in three areas: technical feasibility, licensing, and safety.

Technically, the pump current measurement is preferred over the Gentile ΔP measurement based on the number of assumptions required to support each model. To justify the relationship between current and voiding, the efficiency of the torque transfer at the impeller during two-phase conditions must be quantified. In contrast, the Gentile ΔP measurement requires knowledge of the transfer of torque at the impeller, the energy losses in the diffuser section, the degradation of developed head and capacity, and the enhancement of frictional losses in the RCS during two-phase operation. Consequently, detailed justification of the Gentile ΔP method may be more difficult. Although as shown in Figure 2, Model 2 shows good agreement with the best estimate prediction of actual voids in the system.

With respect to licensing, both models may be acceptable. The NRC is currently supporting the LOFT pump power/current work. They have also given Westinghouse the preliminary approval for a pumps running void measurement based on the ΔP across the reactor vessel. Therefore, these types of measurement correlations are neither new, nor radical, and should be perceived quite favorably by the NRC.

In the future, the proposed void measurement systems may be required to meet 1E equipment qualification requirements in order to be licensable. The ability of either system to meet the guidelines for 1E equipment is beyond the scope of this study since hardware has not been addressed.

The behavior of the void models to fail high in degraded conditions would be conservative if these measurements were used in RC pump trip circuitry (see Appendix for details of the analysis). Therefore, either model could be an effective indicator of primary system inventory and thus would allow clarification of the trip/no trip decision concerning the RC pumps. The potential use of these models in the pump trip circuitry will be discussed in the next section.

5.0 POTENTIAL USE OF INVENTORY MEASUREMENT TECHNIQUES IN PUMP TRIP CIRCUITRY

As explained in Section 1.0, the level of RCS voiding must be known to determine an optimum pump trip time in the event that the primary system pressure drops below the HPI setpoint. To use the proposed models and their associated voiding signals in pump trip circuitry, the following criterion were used:[7]

1. The trip should be delayed sufficiently to allow the HPI to make up the inventory lost for the most probable small breaks.
2. The trip should be based on a void fraction sufficiently large to be outside of the normal noise band associated with $\alpha = 0$ line.
3. The trip void fraction should be sufficiently small such that the trip will occur before pump degradation becomes significant.

Pump current/power tests at LOFT have shown that a setpoint of .15 (15%) void will meet the above criterion. In comparison, since the Gentile flow signal can fluctuate due to other transitory effects, a setpoint somewhat greater than .15 may be desirable to avoid this larger band of noise for the Gentile measurement. This higher setpoint can be justified since SBLOCA analysis indicates that a system can proceed to approximately 0.4 void (40%) before the pumps must be tripped. In any event, either measurement can provide a conservative indication of void which will yield acceptable pump

trip times for small breaks in shich the HPI cannot keep up. When breaks in which the HPI can makeup the inventory being lost or when overcooling events occur, an unnecessary pump trip will be avoided and plant shutdoen will be made more manageable.

A conceptual design for a void measurement system using the Gentile ΔP model would require three inputs:

1. ΔP signal from the Gentile
2. RCS pressure from the wide range taps located on the hot legs.
3. Indication of number of pumps running.

The ΔP signal will be used as the time-varing ΔP_{TP} input and the RCS pressure measurement will be used by a calculating module to determine the saturation properties v_f and v_g. The only unknowns that remain are the calibration constants ΔP_r and v_r. At 100% power with 4 RC pumps running, ΔP_r can be recorded when the Gentile is calibrated using the secondary side heat balance. The reference specific volume can be determined by a calculating module which uses RCS narrow range pressure and loop temperature measurements as inputs. When switching to other modes of RC pump operation, ΔP_r and v_r will have to be updated by an appropriate logic circuit. Five modes of pump operation should be considered:

1. 4 RC pumps on
2. 3 RC pumps on
3. 2 RC pumps on in one loop while the other loop is idle
4. 2 RC pumps on - one in each loop
5. 1 RC pump on

To obtain accurate values of ΔP_r and v_r for each mode, ΔP_r will have to be recorded and v_r will have to be calculated and recorded when the plant is in these modes. In this fashion the date base for the logic circuit is developed.

Similarly, a conceptual design for a void measurement system using pump current would require two inputs:

1. Pump current measurement
2. RCS pressure from the wide range taps located on the hot legs

The current measurement will be used as the time-varying I input and the RCS pressure measurement will be used to estimate the suction pressure at the RC pumps, such that a calculating module can determine the saturation properties ρ_f and ρ_g. The calibration constants I° and ρ° will be recorded using a method similar to the one proposed for the Gentile ΔP system mentioned above. A logic circuit may not be required to account for changes in pump efficiency during various modes of RC pump operation. Furthur development of the concept is required to confirm this.

The void estimates from either of these systems could be coupled with the ESFAS system to provide automatic pump trip.

6.0 CONCLUSIONS AND RECOMMENDATIONS

Two methods for determining RCS voiding have been developed and have been shown to be technically feasible. The first method utilizes the Gentile ΔP signal to infer system voiding. The second method utilizes the RC pump current measurement to determine the inventory of the RCS. Both measurements can produce conservative estimates of voiding to allow for more effective accident management.

Although both the pump current and Gentile ΔP methods are technically feasible, it is recommended that the pump current approach be pursued for further development. This recommendation is based on the following strengths of the pump current approach relative to the Gentile ΔP:

a) Fewer assumptions are required to support the model
b) An experimental data base from scaled pump tests exists
c) The pump current scheme may not require implementation of logic to account for the number of pumps running
d) NRC is familiar with and has indicated acceptance of the principle

REFERENCES

1. "Evaluation of Transient Behavior and Small Reactor Coolant System Breaks in the 177 Fuel Assembly Plant," Babcock & Wilcox Co., May 7, 1979.

2. "Analysis Summary in Support of an Early RC Pump Trip," and "Supplemental Small Break Analysis," submitted as Attachment B to B&W plant Owners Letters in response to NRC Bulletin 79-05C.

3. "Generic Assessment of Delayed Reactor Coolant Pump Trip During Small Break Loss of Coolant Accidents in Pressurized Water Reactors", NUREG-0623, November, 1979.

4. J. W. Murdock, "Two-Phase Flow Measurements with Orifices, " Trans, ASME 84 (4), 419-432, 1962.

5. E. Bizon, "Two-Phase Flow Measurement with Sharp-Edge Orifices and Venturis", AECL-2273, June, 1965.

6. J. F. Ripken, N. Hayakawa, "Calibration Study of a 36 Inch HAMMEL-DAHL Flow Tube (Oconee No. 3), University of Minnestoa St. Anthony Falls Hydraulic Laboratory, Memorandum No. M-125, August, 1970.

7. "Reactor Coolant Pump Motor Power or Current Criteria for Reactor Coolant System Inventory Management in Commercial PWR's During Accidents," LOFT Research Memorandum, March, 1982.

APPENDIX

To give the reader a qualitative "feel" for these models, a simple computer code, VOIDCOM, was developed. VOIDCOM models the RCS as a single homogeneous thermodynamic node. Within this node, conservation of mass is determined by considering the addition of mass due to the HPI system and the loss of mass out of a small break. Conservation of energy is maintained by summing the energy contributions to the RCS via the core, steam generators, HPI system, and the break. By considering the RCS as a fixed volume system, the pressure of this large node can then be determined using the conservation of mass and energy principles. A somewhat pseudo primary loop containing a Gentile flow tube and a RC pump is then superimposed within the RCS thermodynamic node. The mathematical modeling of the Gentile flow tube and the RC pump is of sufficient detail to allow the data presented in Section 3 to be utilized. The output of these component models is a simulated signal of ΔP for the Gentile flow tube and current for the RC pump. The two viable voiding models presented in Section 2 are then applied to yield an estimate of system voiding (via Gentile ΔP and pump current) which can be compared to the thermodynamic voiding of the system which is known.

A TMI-2 type scenario was used to create a voiding transient upon which the models and data could be applied. The chain of events are as follows: (See Figures 13-18)

1. At time zero, the reactor is at 100% power.
2. Loss of all feedwater begins just after time zero.
3. As the steam generators provide less of a heat sink to the primary system, the RCS pressure rises until the PORV lifts. (t = 15 seconds)
4. The PORV sticks open and water continues to flow out of the break.
5. As the RCS pressure drops below the HPI setpoint, the HPI flow is throttled off. (This is done in this example to create significant voiding in a small period of time.)
6. Auxiliary feedwater is valved in and reaches full capacity (t = 4 minutes)
7. At.20 void, HPI flow is reinstated at full capacity (t = 40 minutes)
8. System inventory then recovers and the RCS returns to a subcooled condition. (t = 56.5 minutes)

The transient mentioned was analyzed twice, once assuming non-degraded pump performance, and then a second time assuming that the pump would experience some degradation. In the second analysis, a pump head and torque degradation multiplier was applied which approximates the data presented in Section 3 for the Combustion Engineering data at pressures around 1000 psia. The expressions which were used for the head degradation multiplier, M_H, are as follows:

$$M_H = 1.0 \qquad 0.0 \leq \alpha \leq 0.14$$

$$M_H = 1.4242 - 3.03\,\alpha \qquad 0.14 < \alpha < 0.25$$

Similarly, for the torque degradation multiplier, M_T, the expressions are,

$$M_T = 1.0 \qquad 0.0 \leq \alpha \leq 0.10$$

$$M_T = 1.2 - 2.0\,\alpha \qquad 0.10 < \alpha < 0.25$$

Note the expressions for the multipliers were limited to the range $0 \leq \alpha < 0.25$ due to the dynamics of the problem analyzed.

Review of figures 13 through 18 gives the reader a quantitative feel for the two models presented, and the impact that the pump degradation can have on the resulting estimates of system voiding. With these figures, comparisons can be made which allow the uncertainties associated with each measurement technique to be estimated.

In figure 13, the transient behavior of the RCS system pressure is shown for both the degraded and non-degraded cases. Due to the simplistic nature of the VOIDCOM thermodynamic model, the system pressure is identical for both cases. When a loss of all feedwater occurs, the pressure in the RCS increases from the steady state value until the PORV lifts and sticks open. The pressure then drops until it settles out to a saturation pressure determined by the heat sink provided by the steam generators. At approximately 56.5 minutes, the HPI flow, being greater than the leak flow, has brought the RCS back into a solid condition. The pressure then rises until a pressure level is reached where the leak flow becomes equal to the HPI capacity ($p \approx 2050$ psia).

The loop flow rate versus time is shown in figure 14. In the non-degraded case, the reduction in flow is due to changes in system density only (equation 1, Section 2). By comparison, when the system void exceeds .14, the flow rate is further reduced due to the now degraded pump head (Figure 15). The degradation in flow rate is not large relative to the loss in developed pump head because it is assumed that the flow rate varies as the square root of the ΔP across the pump.

In figure 16, the transient behavior of the hydraulic torque is shown. When non-degraded behavior is assumed, the torque varies as a function of density only. Under degraded conditions ($\alpha > .10$), the transfer of torque becomes less efficient as void increases.

The void estimates predicted using the Gentile ΔP and pump current models assuming non-degraded pump performance are compared to the actual thermodynamic void in figure 17. It can be seen that both models produce good estimates of system voiding. Figure 18 depicts the same estimates assuming pump degradation occurs. For both the Gentile ΔP and pump current method, the degraded pump performances cause the predicted voiding to be overstated.

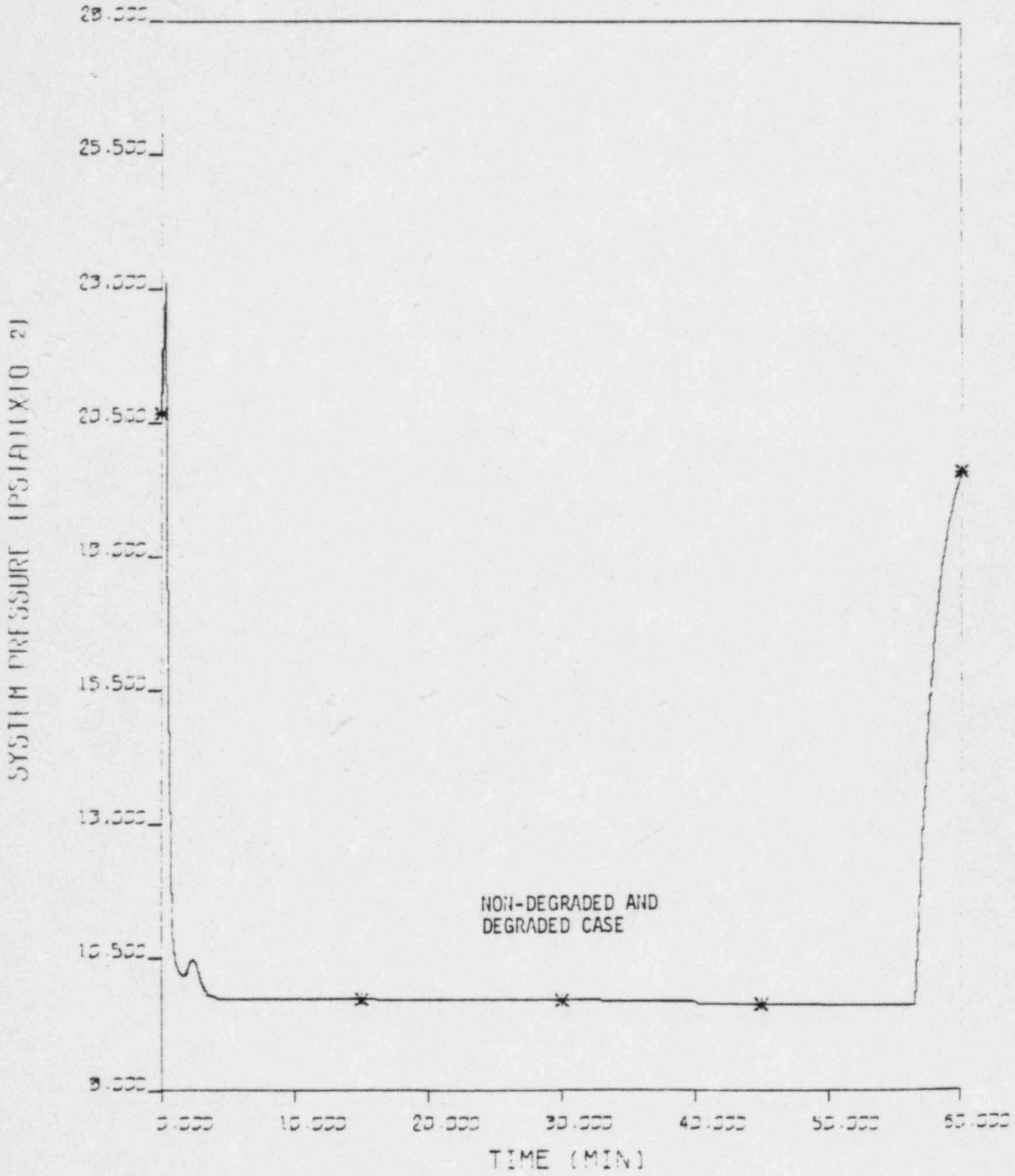

FIGURE 13: SYSTEM PRESSURE VS TIME

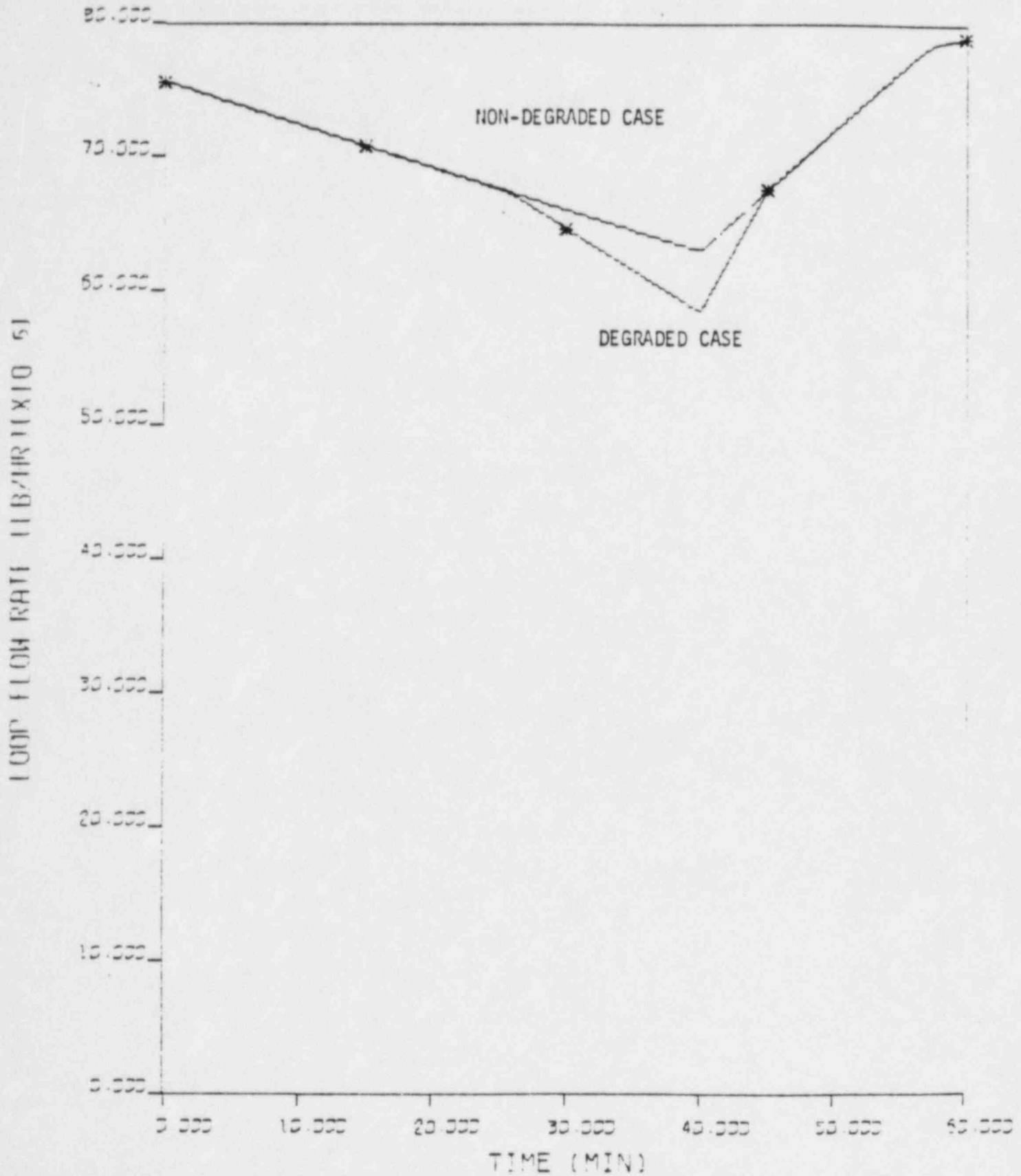

FIGURE 14: LOOP FLOW RATE VS TIME

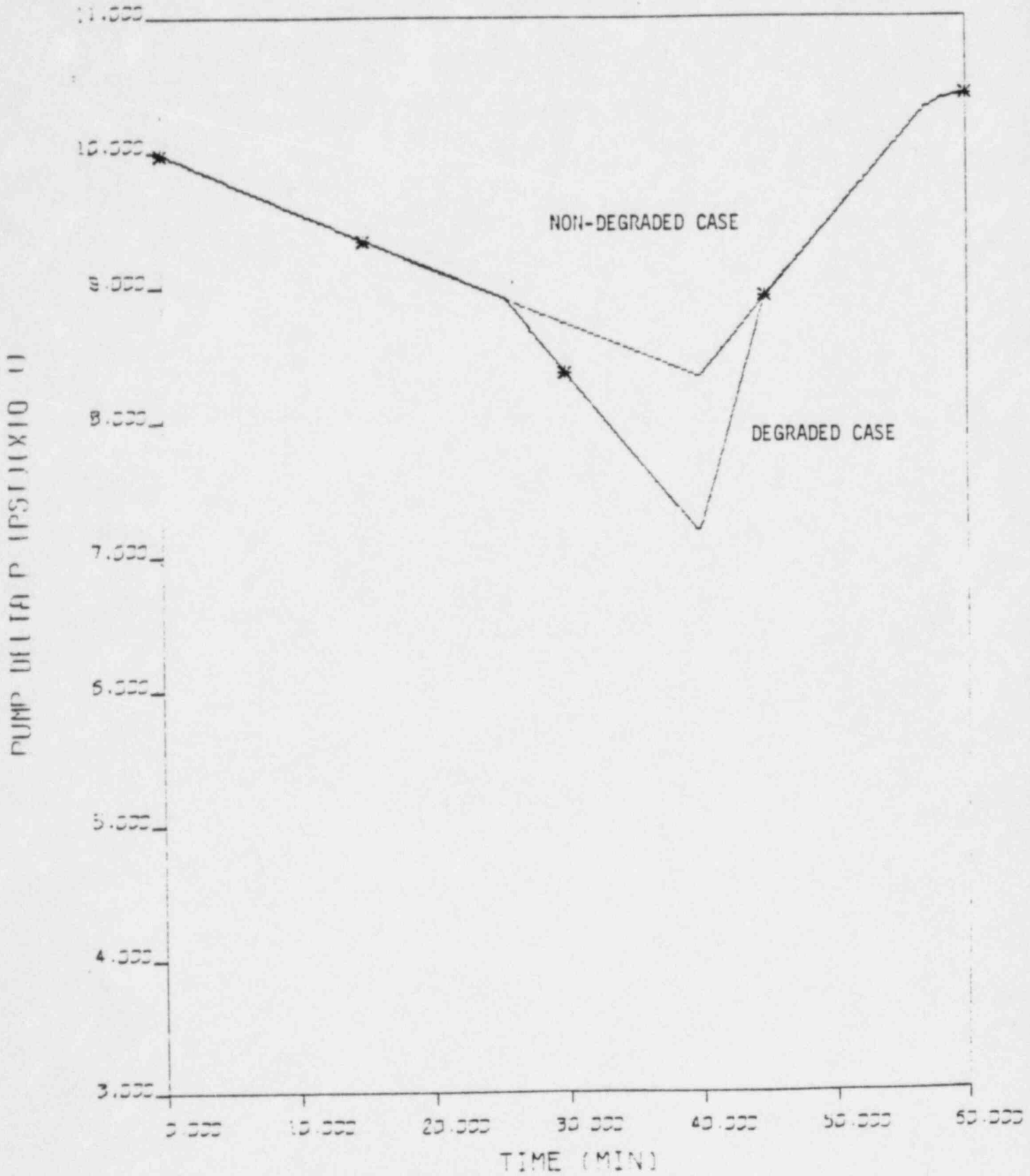

FIGURE 15: PUMP DELTA P VS TIME

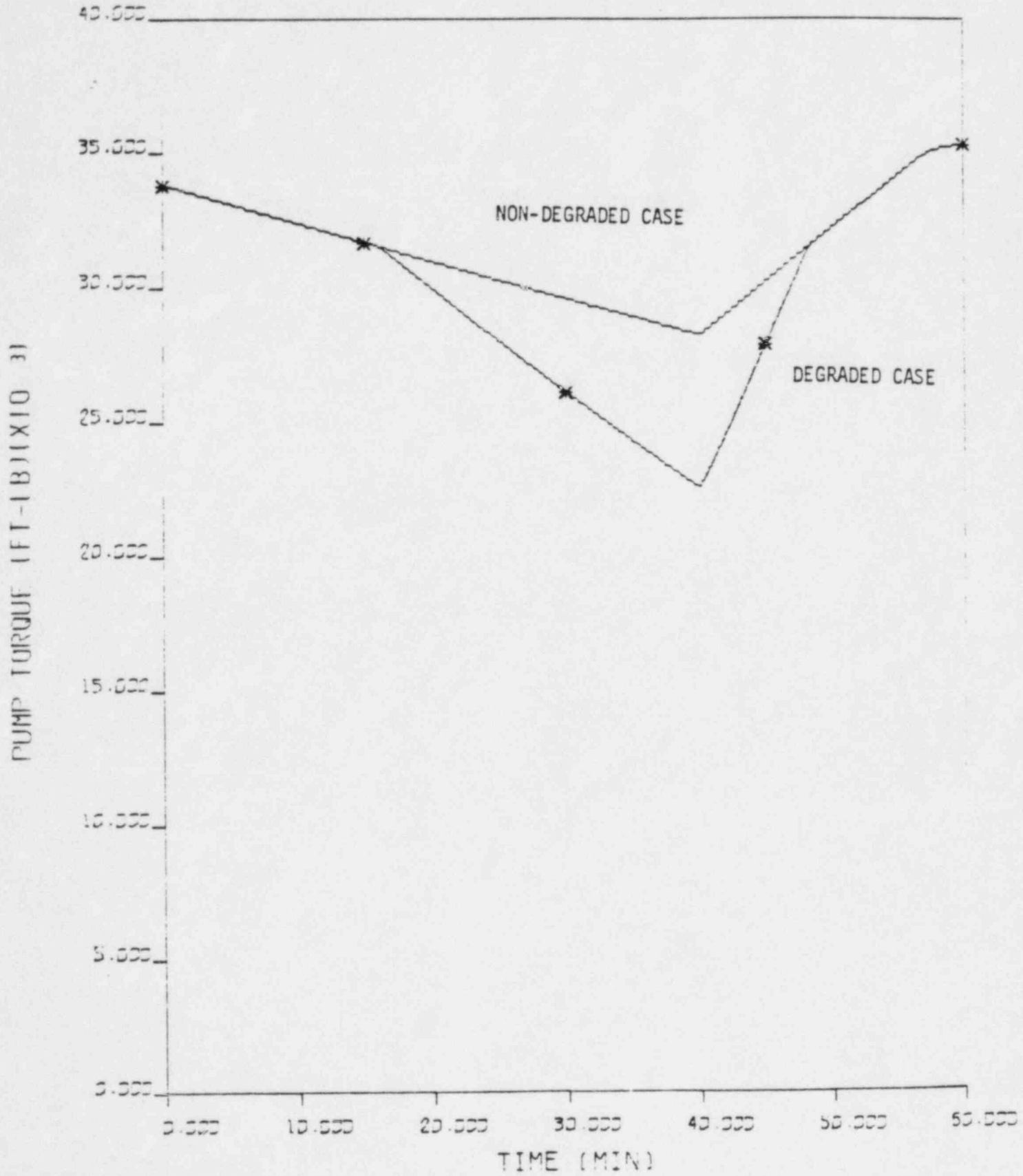

FIGURE 16: PUMP TORQUE VS TIME

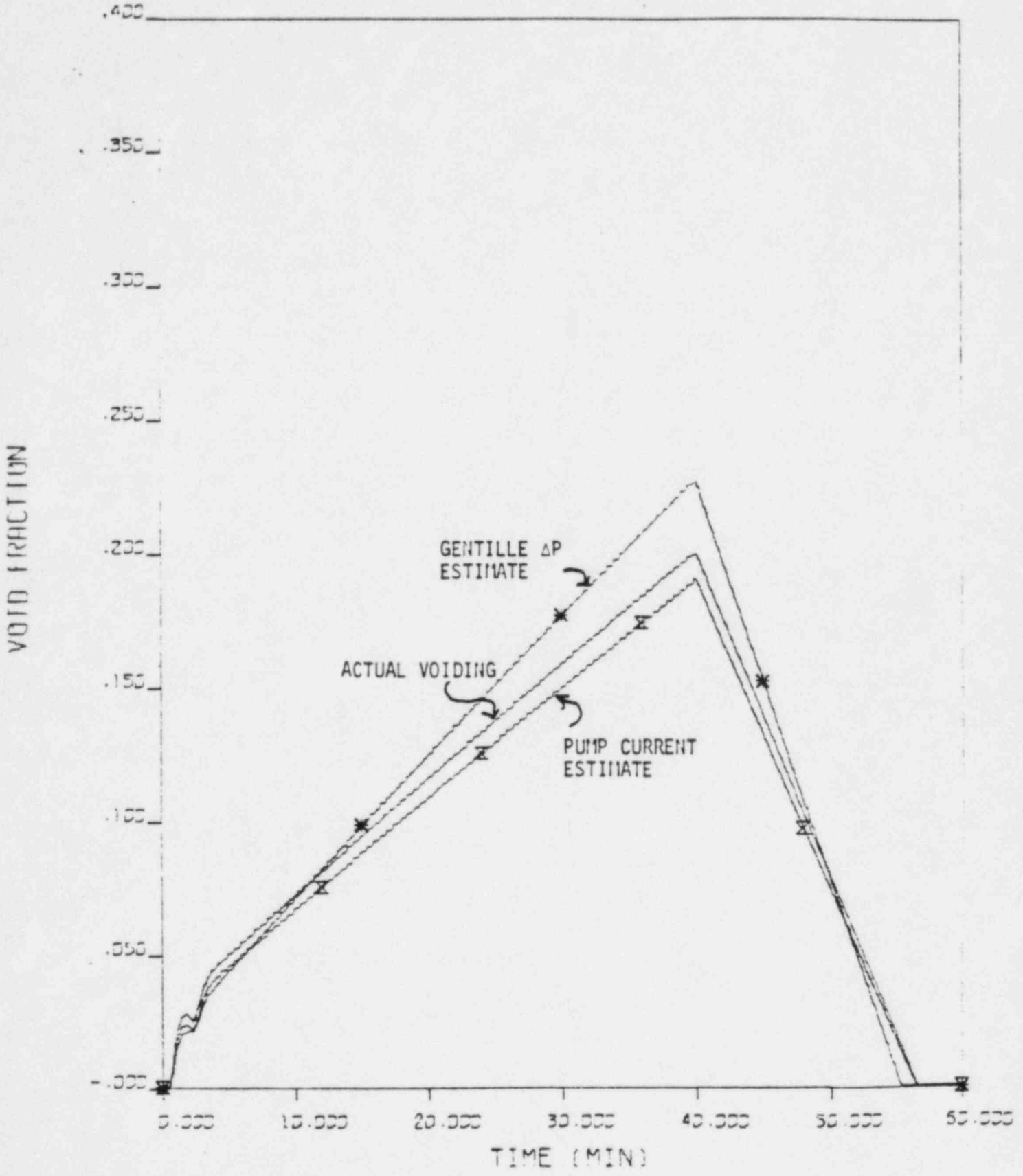

FIGURE 17: VOID FRACTION VS TIME (NON-DEGRADED)

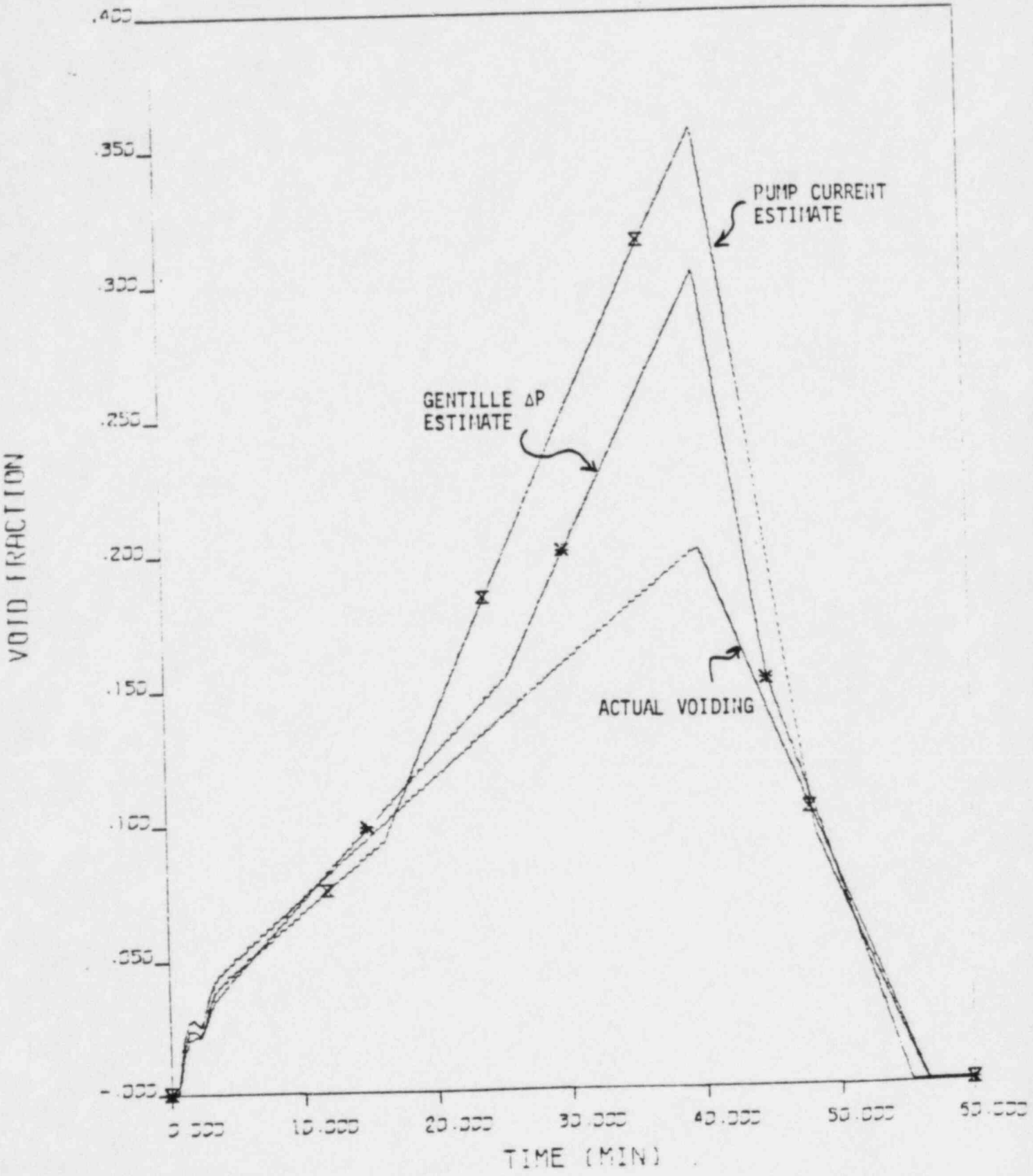

FIGURE 18: VOID FRACTION VS TIME (DEGRADED)